DAMPING OF MATERIALS UNDER

BIAXIAL STRESS

TECHNICAL DOCUMENTARY REPORT NO. ASD-TDR-62-1030

MAY 1963

DIRECTORATE OF MATERIALS AND PROCESSES
AERONAUTICAL SYSTEMS DIVISION
AIR FORCE SYSTEMS COMMAND
WRIGHT-PATTERSON AIR FORCE BASE, OHIO

Project No. 7351, Task No. 735106

NOTICES

When Government drawings, specificatic.1s, or other data are used for any purpose other than in connection with a definitely related Government procurement operation, the United States Government thereby incurs no responsibility nor any obligation whatsoever; and the fact that the Government may have formulated, furnished, or in any way supplied the said drawings, specifications, or other data, is not to be regarded by implication or otherwise as in any manner licensing the holder or any other person or corporation, or conveying any rights or permission to manufacture, use, or sell any patented invention that may in any way be related thereto.

Qualified requesters may obtain copies of this report from the Armed Services Technical Information Agency, (ASTIA), Arlington Hall Station, Arlington 12, Virginia.

This report has been released to the Office of Technical Services, U.S. Department of Commerce, Washington 25, D.C., for sale to the general public.

Copies of this report should not be returned to the Aeronautical Systems Division unless return is required by security considerations, contractual obligations, or notice on a specific document.

C

FOREWORD

This report was prepared by the Department of Aeronautics and Engineering Mechanics of the University of Minnesota under USAF Contract No. AF 33(657)-7453. This contract was initiated under Project No. 7351, "Metallic Materials", Task No. 735106, "Behavior of Metals". The work was administered under the direction of the Metals and Ceramics Laboratory, Directorate of Materials and Processes, Deputy for Technology, Aeronautical Systems Division, with Mr. D. M. Forney, Jr. acting as project engineer.

This report covers work conducted from 1 January 1961 to 1 August 1962.

The authors would like to express their appreciation of the efforts of Mr. D. Beste, who performed many of the experiments and assisted in the preparation of this report; and of the helpful comments and suggestions by Dr. R. Plunkett. The manuscript preparation was by Judith Graf.

ABSTRACT

A new theory of combined stress damping is developed and evaluated on the basis of experimental results for several materials. It is concluded that the new theory should be limited in application to materials whose dominant damping mechanism is known to be plastic deformation. It appears that a separate theory of combined stress damping may be required for each mechanism of damping.

This technical documentary report has been reviewed and is approved.

W. J. TRAPP
Chief, Strength and Dynamics Branch
Metals and Ceramics Laboratory
Directorate of Materials and Processes

iii

TABLE OF CONTENTS

LIST OF FIGURES

I. INTRODUCTION

The importance of material and structural damping as a means of controlling the amplitude of resonant vibrations in members and configurations subjected to cyclic loads has been discussed in several prior publications (1) (2), and summarized in reference (3). The early investigations of damping were naturally concerned with the common engineering materials when subjected to the simple states of stress as obtained under bending, torsional or axial loadings. The damping properties of many materials have been experimentally determined for these loadings, and the effects of other variables such as stress history, temperature and frequency of loading considered.

As material damping began to emerge as an important factor in the controlling of resonant fatigue, several new alloys displaying high damping capacities were developed and have been used, to some extent, for this purpose. Notable among these are the manganese copper alloys, some reinforced plastics, and materials exhibiting large magnetoelastic damping. In structural application, however, it is frequently found that states of stress occur which are more complicated than in simply loaded test specimens, and thus an experimental determination of the damping properties of materials subjected to all possible states of combined stress would be desirable. This would be a formidable task. It might rather be more productive to seek to establish laws, or criteria, which would be useful for predicting the damping properties of materials under combined stress.

As a result, the following goals have been chosen for this investigation:

1. To establish a procedure for predicting the damping properties of materials under various states of combined stress from known damping properties under uniaxial stress conditions.

2. To determine experimentally the damping capacities of several materials over a range of combined stresses in order to verify the validity of any procedure established under 1.

---

* Numbers in parentheses refer to a bibliography on page 21.

II. REVIEW OF PRIOR WORK ON COMBINED STRESS DAMPING

Robertson and Yorgiadis (4) compared the damping of several materials under axial and torsional loadings, and found that the ratio of axial to torsional stress necessary to produce the same damping ranged from 0.48 to 0.60. They also cite data obtained by Foppl, who determined this factor to be between 0.53 and 0.60 for several steels. These similarities between various materials suggest the existence of a general rule or criteria of combined stress damping. As a ratio of torsional to axial stress of 0.577 is required to produce the same distortional energy, Robertson and Yorgiadis were led to the conclusion that states of stress displaying equal distortional energies should display equal damping.

V. W. Anderson (5) conducted tests on hollow tubes of mild steel and pure copper at various states of biaxial stress. The specimens were subjected to a completely reversed tension-compression load cycled in phase with an alternating torsional load. Because of the large magnitudes of stress found necessary to produce measurable damping, his data may have been affected to some extent by stress history, but certain meaningful trends are evident. He found the damping of mild steel under any state of combined stress (obtainable by a simultaneous application of axial and torsional loads) to be reasonably close to the damping which would be measured in a specimen of the same material subjected to an axial stress of magnitude sufficient to produce the same octahedral shearing stress. Under the same conditions, pure copper was found to have approximately the same magnitude of unit damping as would be found in a specimen subjected to the uniaxial stress necessary to produce the same strain energy. Some results of Anderson's investigations are presented graphically in Figures 1, 2 and 3. The basis of this investigation was the assumption that corresponding to any state of combined stress there is a uniaxial stress (the equivalent stress) which will produce the same damping. This approach will hereafter be termed an equivalent stress theory. The equivalent stresses considered w.re defined by equating various quantities, such as the maximum principal stress, the maximum strain, the maximum shear, the maximum distortion energy, and the maximum strain energy. The resulting equivalent states of stress are as indicated in Figure 4. Several curve fitting techniques were developed and employed to ascertain which of these criteria would best describe the combined stress damping properties of each material.

J. S. Whittier (6) proposed that the unit damping under a state of combined stress could be bounded above by the damping which would occur if the damping were due only to dilatation, and below by the damping due only to distortion. The data of Robertson and Yorgiadis, Foppl, and Anderson do not appear to fall entirely within these bounds; however, Whittier suggests that this may have been

2

due to anisotropy. In an experiment carefully designed to minimize the effects of anisotropy and stress history, Whittier found the damping of mild steel under a biaxial state of stress to be nearly midway on a logarithmic plot between the proposed bounds. He obtained a state of biaxial stress by vibrating a circular plate in its umbrella, or first-free mode. One important feature of any bounding technique is the ratio of the bounds, which in Whittier's work was approximately seven to one. This ratio is fairly large in comparison with the standard deviation of damping values encountered in typical investigations. In an effort to improve the accuracy of prediction, Whittier considered the ad hoc possibility that the two modes of dissipation might be equally effective. This led to predicted values within 150% of the measured values.

III. A NEW THEORY OF COMBINED STRESS FOR DAMPING

It is the purpose of a combined stress theory to predict the magnitude of a simple uniaxial stress, such as tension, which will produce the same material behavior as a given state of combined stress. Such phenomena as yield, fatigue, creep, and damping may all be of interest in a member subjected to a multiaxial state of stress.

Historically, the first of these to be considered both experimentally and analytically was yield, and it has been generally found that ductile materials will yield as predicted by either the Tresca or Von Mises criterion. The Tresca yield condition assumes that yield will begin when the maximum shearing stress reaches a certain critical value. V n Mises' criterion, (critical magnitude of the second deviatoric invariant), the distortion energy theory, (critical level of the energy of distortion), and the maximum octahedral shearing stress(max OSS)theory, (critical level of OSS), all predict the same yield locus, although they differ somewhat in their formulations. It is of interest to note that the above mentioned theories all predict that yield will not be produced by any amount of hydrostatic pressure or dilatation. Other yield theories in common usage which do permit some influence of dilatation on yield are the maximum stress, maximum strain and the maximum strain energy theories. All of these theories, as applied to yield, are discussed more fully in references (5 and 7). These theories of combined stress have also been applied to other phenomena by means of equivalent stresses. Fatigue (7) and damping (5) have been treated in this manner.

A combined stress theory might be defined as the mathematical description of a surface in a coordinate space defined by the three principal stresses, each point of which is equivalent with respect to the phenomenon of interest. For example, in a theory of yield

3

we seek to define the surface which is the locus of all points where yield will commence on the first loading from a virgin state. For damping, the desired surface will contain all points having the same unit damping energy. It is of course possible that two or more phenomena might have the same representation. If, for example, a material exists which displays the same damping at every possible first-yield state, then this yield surface is obviously one of the iso-damping surfaces.

If a material has a locus of points in stress-space characterized by equal damping, then all that will be required for the prediction of the combined stress damping properties is two sets of information:

1. the damping/stress relationship under a simple state of stress,

2. the shape of the iso-damping surfaces.

3.1 Theory

In an earlier investigation of damping under uniaxial stress, Lazan (8) found that the damping could be expressed reasonably well by

$$D_u = K \, \sigma_u \, \mathcal{E}_u'', \tag{1}$$

where

D_u is the specific or unit uniaxial damping energy, having dimensions of $in\text{-}lb/in^3/cycle$, and is the energy dissipated by a unit volume of a homogeneous material during one complete reversal of a homogeneous and uniaxial state of stress;

σ_u is the magnitude of the uniaxial stress;

$\mathcal{E}_u''$ is the magnitude of plastic strain in the direction of the load;

and K is a factor of proportionality depending solely upon the shape of the hysteresis loop.

A hysteresis loop typical of metals is as shown in Figure 5. It will now be asserted that for any given material, the same basic mechanism of damping will be operative at all states of stress.

In an attempt to extend a result observed to be true for uniaxial states of stress, (Eq. 1), to states of biaxial stress, it will

4

be assumed that

$$D(\sigma_1, \sigma_2) = K_1 \sigma_1 \varepsilon_1'' + K_2 \sigma_2 \varepsilon_2'' \tag{2}$$

where

$D(\sigma_1, \sigma_2)$ is the unit damping energy at a state of cyclic combined stress having principal stresses, σ_1 and σ_2 constant in direction and varying sinusoidally with a common period and phase, the third principal stress being always zero;

$\varepsilon_1'', \varepsilon_2''$ are the plastic (non recoverable) components of the principal strains;

σ_1, σ_2 are the greater and lesser principal stresses respectively, and

K_1, K_2 are again hysteresis loop shape factors which, for isotropic materials, will normally be equal.

The form of Eq. 2 implies that no interaction occurs. That is, if σ_1 and ε_1'' are held fixed and ε_2'' is zero, a change in σ_2 will not affect the damping. It is now assumed that the hysteresis loops may be described by

$$\varepsilon_1'' = \Gamma_1(\sigma_1, \sigma_2) \varepsilon_1 \tag{3}$$

and

$$\varepsilon_2'' = \Gamma_2(\sigma_1, \sigma_2) \varepsilon_2,$$

where the $\Gamma_{1,2}$ are functions of the state and magnitude of stress, and will be taken to be equal for an isotropic material. Thus

$$D(\sigma_1, \sigma_2) = K \Gamma(\sigma_1, \sigma_2) \left\{ \sigma_1 \varepsilon_1 + \sigma_2 \varepsilon_2 \right\} \tag{4}$$

This equation predicts that the unit damping energy will be proportional to a product of the strain energy and a function of the state of stress. If the elastic strains are much greater than the plastic strains,

$$\varepsilon_1' \gg \varepsilon_1'' \quad , \quad \varepsilon_2' \gg \varepsilon_2''$$

then $\varepsilon_1' \cong \varepsilon_1$, $\varepsilon_2' \cong \varepsilon_2$.   Employing Hooke's law,

$$E \varepsilon_1 = \sigma_1 - \nu \sigma_2 \quad \text{and} \quad E \varepsilon_2 = \sigma_2 - \nu \sigma_1, \tag{5}$$

5

a substitution into Eq. 4 gives,

$$D(\sigma_1, \sigma_2) = \frac{K}{E} \Gamma(\sigma_1, \sigma_2) \left\{ \sigma_1^2 - 2\nu \sigma_1 \sigma_2 + \sigma_2^2 \right\}. \tag{6}$$

If a new parameter α is introduced such that

$$\alpha = \frac{\sigma_2}{\sigma_1}$$

the loading is then described by the two parameters, α and σ_1, where α specifies the type of loading and σ_1 the magnitude. Then

$$D(\sigma_1, \sigma_2) = \frac{K}{E} \Gamma(\sigma_1, \sigma_2) \, \sigma_1^2 \left\{ 1 - 2\nu \alpha + \alpha^2 \right\}. \tag{7}$$

In order to evaluate the function Γ in terms of the state of stress, we first consider a uniaxial state of stress in a material which has damping properties described by (1, 2)

$$D_u = J \sigma_u^n \tag{8}$$

where J and n are parameters of the material and are dependent upon stress history.

Thus

$$D_u = D(\sigma_1, 0) = D(\sigma_u, 0)$$

or

$$J \sigma_u^n = D(\sigma_u, 0) = \frac{K}{E} \Gamma(\sigma_u, 0) \sigma_u^2$$

and hence

$$\Gamma(\sigma_u, 0) = \frac{JE}{K} \sigma_u^{n-2} \tag{9}$$

If at any state of combined stress the σ_u is replaced by some function σ_* of the principal stresses, σ_1 and σ_2, then

6

$$\Gamma(\sigma_1,\sigma_2) = \frac{JE}{K} \; \sigma_*^{n-2}(\sigma_1,\sigma_2)$$

and

$$D(\sigma_1,\sigma_2) = J\sigma_1^2 \; \sigma_*^{n-2}(\sigma_1,\sigma_2)\left\{1-2\nu\alpha+\alpha^2\right\}.$$

$$(10)$$

As a consequence of these assumptions, it is to be noted that in a material where n is nearly 2, the damping will be proportional to the strain energy, where the factor of proportionality is a slowly varying function of stress. If on the other hand the value of n is very large, the damping will behave as would be predicted by an equivalent stress theory. That is to say, for large n, the combined stress damping $D(\sigma_1,\sigma_2)$ will be dominated by the function σ_*.

The function σ_* (assumed to be a function of the state of stress only) might well be some combination of stress which describes a critical physical quantity, such as:

1. the maximum stress,

2. the maximum strain,

3. the maximum shear, or

4. the maximum octahedral shearing stress.

The representation of these particular quantities in terms of the principal stresses is in some cases dependent upon the signs of the stresses. In the portion of the $\sigma_1 - \sigma_2$ plane attainable under a combined axial and torsional loading, they become

1. $\sigma_* = \sigma_1$ $\qquad\qquad\qquad\qquad\qquad\qquad$ (11)

2. $\sigma_* = \sigma_1 - \nu\sigma_2$ $\qquad\qquad\qquad\qquad\qquad$ (12)

3. $\sigma_* = \sigma_1 - \sigma_2$ $\quad$ and $\qquad\qquad\qquad$ (13)

4. $\sigma_* = \sqrt{\sigma_1^2 - \sigma_1\sigma_2 + \sigma_2^2}$ respectively. $\qquad$ (14)

It is certainly possible to make other assumptions as to the critical physical quantities used to define σ_*, however the ones here chosen are felt to be representative. We thus find the following possible expressions for the Γ function.

1. $\Gamma(\sigma_1,\sigma_2) = EJ/K \; \sigma_1^{n-2}$ $\qquad\qquad\qquad$ (15)

2. $\Gamma(\sigma_1,\sigma_2) = EJ/K \; \sigma_1^{n-2}(1-\nu\alpha)^{n-2}$ $\qquad$ (16)

3. $\Gamma(\sigma_1,\sigma_2) = EJ/K \; \sigma_1^{n-2}(1-\alpha)^{n-2}$ $\qquad$ (17)

$$4. \quad \Gamma(\sigma_1, \sigma_2) = \frac{E J}{K} \, \sigma_1^{n-2} \, (1 - \alpha + \alpha^2)^{\frac{n-2}{2}} \tag{18}$$

The combination of these functions and Eq. (7), the expression for $D(\sigma_1, \sigma_2)$, leads to the nondimensional iso-damping lines shown in Figures 6 and 7. It is interesting to note that the theory is so constructed that for $n = 2$ all curves coalesce to the same iso-damping line and that this iso-damping curve is also the locus of all points having the same strain energy.

The expressions for the functions, σ_*, Γ and $D(\sigma_1, \sigma_2)$ for the various σ_*, are summarized in Table A.

3.2 Discussion

Certain features of this theory should be amplified. The analysis assumes that the sole difference between a state of uni-axial stress and a state of biaxial stress is the state of stress itself. That is, it is implied that the basic mechanism of damping will be the same, and that the effect of such variables as temperature, frequency and metallurgical condition will also be the same in biaxial and uniaxial states of stress. Although the $\Gamma(\sigma_1, \sigma_2)$ is not permitted to vary with the number of cycles of reversed stress, (a stress history effect), the analysis is not restricted to applications where stress history does not appear. The factor J in Eq. (10) may be permitted to vary with n, but only in the same manner as in a uniaxial test. Thus, this theory in-directly predicts that the stress history effects in a combined stress test will be the same as in a uniaxial test.

The restriction to small plastic strains is perhaps more severe. As a measure of smallness, consider the ratio of plastic to elastic strains in a uniaxial test,

$$R = \frac{\varepsilon''}{\varepsilon'}, \tag{19}$$

which is assumed to be small.

Substituting Eq. (1) for the plastic strain and $\frac{\sigma}{E}$ for the elastic, we find that

$$R = \frac{DE}{K\sigma^2} \tag{20}$$

If K is assumed to be three (Ref. 8), the value of R may be computed for various materials as follows (Data taken from Ref. 9).

Material	D	σ_c	E	R
Sandvi' QT	2.8	100,000	29.2	2.72×10^{-3}
Sandvik N	1.3	55,000	29.2	4.17×10^{-3}
N 155	0.4	33,000	30.0	3.68×10^{-3}
1020	0.45	30,000	29.4	4.9×10^{-3}
24ST4	0.45	24,000	10.6	2.77×10^{-3}
Jl magnesium	0.1	8,000	6.5	3.39×10^{-3}
Grey-Iron	0.7	6,500	20.0	.111

The stress level, σ_c , used in these computations is termed the
cyclic stress sensitivity limit, and is that stress level where
stress history first affects damping. This quantity has been pre-
viously discussed by Lazan (1), and is generally less than the
fatigue strength (about 80%, Ref. 2). At the fatigue strength, the
following values were found, using the largest value of damping
which may occur at this stress.

Material	D	σ_e	E	R
Sandvik QT	2.3	92,000	29.2	2.64×10^{-3}
Sandvik N	10-70	76,000	29.2	.118
N 155	26-45	53,000	30.0	.160
1020	0.7-20	35,500	29.4	.156
24ST4	0.6-10	27,000	10.6	.0475
Jl magnesium	0.5-1.3	17,000	6.5	.00976
Grey-Iron	1.3-1.9	9,500	70.0	.141

As a consequence of the above, it may be seen that the assumption
of negligible plastic strains in comparison with the elastic strains
is quite valid at the stress sensitivity limit, at least for ma-
terials such as these, but may be questionable at stresses at or
above the fatigue strength. For most materials the ratio R will
increase, and in many cases quite rapidly, as the stress is raised
above the sensitivity limit, σ_c .

This theory bears certain resemblances to the equivalent stress
theory as previously described. If n = 2, this theory, regardless
of the choice of σ_* , is identical to an equivalent stress theory
based upon equivalent strain energies. For very large n, this
theory coincides with the equivalent stress theories, where the σ_*
becomes the equivalent stress.

A prediction of an effect of dilatation on damping is built into this theory. Since the damping is found to be proportional to the strain energy, and the strain energy not independent of dilatation, it follows that the damping will depend also on the dilatational component of the stress tensor. This is perhaps one of the greater qualitative differences between this theory and an equivalent stress theory based upon the Von Mises yield condition. It is to be recalled that the experiments of J. S. Whittier (6) showed a pronounced effect of dilatation on combined stress damping.

3.3 Application of The New Theory to Previously Obtained Results

The data of V. W. Anderson (5), Figure 3, appear as indicated in Figure 8 (mild steel) and Figure 9, (pure copper), when reduced to a dimensionless form. The lines of iso-damping as predicted by the various equivalent stress theories are indicated on these figures. From the original data obtained by Anderson, the slope of the log damping vs. log stress curve, n, is found to be between 7.5 and 11 for mild steel, and between 3.2 and 3.8 for pure copper. For representative values of n, (9 and 3.5), the theory developed in the preceding section predicts the iso-damping lines of Figures 10 and 11 respectively. Anderson's data are plotted again on these figures, and it may be seen that the new theory gives a reasonable description of the combined stress damping behavior if the critical physical quantity, σ_* , is chosen as either maximum shear or distortional energy in the case of m'ld steel, and as the maximum strain for pure copper.

Apparently this new theory is adequate for the description of the combined stress damping behavi·: of these materials. It might now be pertinent to attempt to apply this theory to materials with different basic damping mechanisms in an effort to discover if this theory is limited in application to materials of specific mechanisms.

IV. EXPERIMENTAL INVESTIGATION

4.1 Description of the Biaxial Stress Damping Machine

The biaxial stress damping machine used in this investigation was designed and constructed by V. W. Anderson and has been previously described by him (5). A schematic diagram of the machine is presented as Figure 12, and a brief description of the mechanism is as follows. By means of crank mechanisms, axial loads of up to +4200 pounds and torques of up to +1000 in-pounds may be applied to a thin-walled cylindrical specimen. The cyclic axial load is applied to the specimen S through a vertical shaft which in turn is connected to one end of lever arm A by a flex plate. The lever A can move only in the vertical plane. A connecting rod and variable throw crank assembly V_1 are attached to the opposite end of lever A.

10

By changing the throw of the crank, which may be done while the machine is in motion, the magnitude of the cyclic load applied to S may be increased or decreased. The torsional load is applied in a similar manner through an identical variable throw crank assembly V_2 as shown in the top view of Figure 12. The variable throw crank for the torsional load is linked to the same vertical shaft by means of a connecting rod and a torque arm T. This torque arm may move only in the horizontal plane. By changing the throw of V_2, as may be done while the machine is in motion, the torque acting on S may be adjusted. The crank settings of V_1 and V_2 as well as the number of cycles of alternating stress are noted by revolution counters attached to the machine. Timing belts connect V_1 and V_2 through a speed reducer to a controllable speed motor. By means of a timing belt between V_1 and V_2, the phase between the axial and torsional loads may be adjusted.

The axial and torsional loads are measured by a dynamometer D which employs resistance type strain gages to sense the changes in force and torque. The location of gages and circuitry were chosen so that the axial and torsional loads would be measured independently of each other. Axial and torsional strains in the specimen S are also measured independently by means of resistance type strain gages attached to the specimen.

4.2 Instrumentation and Calibration

The measuring and recording instrumentation consisted of the following elements: an X-Y Autograph recorder, switch box, stress and strain control boxes, dynamometer, resistance strain gages on the specimen, and a voltage supply. These elements were assembled as indicated in Figure 13. Stress-strain hysteresis loops were plotted on the recorder for any combination of alternating axial and torsional stresses. A switch box was included in the circuit such that torsional and axial hysteresis loops might be plotted with the same recorder.

The dynamometer was calibrated by determining the load required to produce the same recorder deflection as a precision resistor shunted into the dynamometer circuit. A range of resistor sizes was used to insure a valid calibration over a wide range of loads. This method of calibration is independent of long term battery voltage drift or recorder adjustment. A similar procedure was employed in the torsional load calibration, the loads necessary for calibration being obtained by attaching dead weights to the torsion arm. Again, several precision resistors corresponding to a wide range of torsional loads were used.

The axial strain in the specimen was calibrated by relating the strain reading of a Tuckerman Optical Extensometer to a precision resistor shunted across one arm of a Wheatstone bridge.

11

Finally, the torsional strain was calibrated analytically from the relationship,

$$\mathcal{E}_s = \frac{R}{\lambda(R_s + R)}, \tag{21}$$

where $\mathcal{E}_s$ is the torsional strain,

R_s is the known shunt resistance,

R is the known resistance of the electric gage,

and λ is the gage factor.

The calibration factors for strain measurement have been checked periodically to insure uniformity in the strain readings obtained from various specimens.

4.3 The Experimental Program

One of the goals of this investigation was to determine the damping values of selected materials over ranges of stress magnitudes and principal stress ratios. The testing machine previously described was used as it is capable of producing any combination of principal stresses in the range

$$0 \leq -\sigma_2 \leq \sigma_1 \quad \text{for} \quad \sigma_1 > 0, \text{and} \quad 0 \leq \sigma_2 \leq -\sigma_1 \quad \text{for} \quad \sigma_1 < 0.$$

Since the means of damping evaluation employed was the direct measurement of hysteresis loop areas, it was necessary to confine the investigation to states of stress which would produce hysteresis loops of sufficient area to be measurable with a planimeter. On the other hand, it was desirable to conduct the experiments at stresses below the point, σ_c, where damping capacity would be affected by the number of cycles of stress. A material such as mild steel does not display a hysteresis loop of significant width below this limit, and consequently, to measure loops of the aforementioned material by this method, it would be necessary to operate at levels of stress above σ_c, and stress history effects could become serious.

This would not be feasible in this investigation, as it would necessitate the use of a separate specimen for each stress ratio to be tested. Thus, a material is required which will have high damping at stresses below stress σ_c. In order to define exactly what is meant by "high", a material parameter descriptive of this property is needed. Since the hysteresis loops are in any case quite narrow, they were assumed to be very narrow ellipses. The area of an ellipse is π times the product of the semi-major and semi-minor axes. Consequently, solving for the semi-major and minor axes

12

in terms of the maximum stress and strain in the cycle, it is found that

$$\rho = \frac{D_1 E_{s1}}{2\pi \sigma_1^2}$$ (22)

where $\rho = \dfrac{\text{width of loop (in direction of minor axes)}}{\text{length of loop (in direction of major axes)}} = \dfrac{1}{2}$ (loss factor),

$D_1 =$ damping energy associated with a stress level σ_1 ,

$E_{s1} =$ is the secant modulus associated with a stress level σ_1 ,

and $\sigma_1 =$ is the level of uniaxial reversed stress.

A hysteresis loop where ρ is about 1% was found to be the narrowest which could be measured by a planimeter with any degree of accuracy. The quantity defined by Eq. (22) is very similar to the ratio defined by Eq. (20). In fact,

$$\rho = \frac{K}{2\pi} \frac{E_s}{E} R .$$ (23)

If the analysis of Section III is to apply, R must be small, certainly no more than 0.1. Thus, the most desirable material is one having a value of ρ between 1% and 5% at a stress less than σ_c .

4.4 Description of Materials and Test Members

The specimens used in the experiments were made from bar stock of manganese copper (CDC #780, Chicago Development Corporation, 5810 - 47th Avenue, Riverdale, Maryland) and Cobalt Nickel (Nivco 10, Westinghouse Electric Corporation, Blairsville, Pennsylvania) alloys. The chemical compositions of these alloys were stated by the manufacturers to be:

Nivco 10

Element	Range (% Composition)
C	0.05 Max
Mn	0.20-0.50
Si	0.10-0.25
P	0.01 Max
S	0.02 Max
Fe	1.00 Max
Al	0.15-0.30
Ti	1.55-1.95
Zr	0.90-1.20
Ni	21.50-23.50
Co	Balance

13

CDC #780

Element	Range (% Composition)
Mn	78-82
Cu	18-22.

Some of the mechanical properties of these alloys at room temperature are:

Nivco 10

Fatigue strength	52,000 psi at 10^8 cycles
Modulus of elasticity	29.7 x 10^6 psi
0.2% Yield strength	110,000 psi

CDC #780

Fatigue strength	17,000 psi at 10^8 cycles
Modulus of elasticity	13.5 x 10^6 psi
0.2% Yield strength	24,000 psi.

These materials were chosen primarily for their high damping properties at low stress levels produced by mechanisms other than plastic deformation. The effect of stress history on the damping of manganese copper was previously found to be very small (10). The relative damping values of these materials under reversed loading are compared with other structural materials in Figure 14. Both materials were heat treated by the manufacturers to insure the maximum isotropy necessary for a unique relationship between uniaxial and biaxial damping properties.

In order to minimize the inevitable variation of properties from specimen to specimen, all specimens of each material were cut from the same bar. All of the specimens were of the thin walled cylindrical type designated as "Type ND" and shown in Figure 15. The ratio of the wall thickness to the diameter of the specimen is about 0.027, which is small enough to assure a nearly uniform distribution of shear stress over the cross sectional area. The outside diameter and the length of the test section provide an adequate surface for the fastening of the resistance type strain gages used to measure axial and torsional strains. The effects of specimen fillets on strain readings were assumed to be negligible, since the fillets are of a large radius and the strain gages mounted well away from them. Machining and polishing procedures were identical to those previously described (11).

14

4.5 Test Procedure

Previous investigators have found that the unit damping energy for a given material, frequency and temperature depends both on stress amplitude and stress history. Combined axial and torsional damping tests were conducted so as to minimize the effect of stress history. As a check on the effect of stress history on the specific damping energy, the following experiment was conducted. The specific damping energy was determined at a minimum stress level σ_L, and at increasing stress levels until a maximum stress amplitude, σ_m was reached. Then the damping was measured at decreasing amplitudes of stress until the minimum value was reached. This experiment again was conducted for both pure axial and pure torsional loadings. The results are as shown in Figure 16. This preliminary test indicated that there was some range of stress over which no appreciable stress history effect would occur when the loading was either pure axial or pure torsional. It then becomes plausible to assume that no stress history effect will exist over a similar range of equivalent stresses when the loading is a biaxial combination of axial and torsional loads. This was indeed found to be the case. For each value of α used, the damping vs. measure of stress curve retraced well when the magnitude of σ_1 was increased and subsequently decreased within a range $\sigma_L < \sigma_1 < \sigma_m$.

To accomplish the second of the objectives outlined in the introduction, the following procedure was established.

1. Several levels of stress σ_1, all such that $\sigma_L < \sigma_1 < \sigma_m$ were chosen.

2. Several combinations of axial and torsional loadings were selected.

3. At each combination in (2), the loading program (1) was carried out with a sufficient number of repeat runs to establish reproducibility.

4. 1 through 3 were repeated with a different specimen.

The specimen was secured in the proper neutral position on the biaxial stress damping machine by eliminating nearly all axial or torsional pre-load from the specimen. By using the recording apparatus at maximum sensitivity, it was found possible to eliminate axial and torsional stresses to within 100 psi. Care was exercised in specimen alignment to insure that no bending stress would be introduced.

Duplicate hysteresis loops were recorded to check their reproducibility. All damping tests were performed at room temperature and at a frequency of 4 cycles per minute, a convenient speed at which to operate the X-Y recorder.

15

4.6 Data Reduction

The test specimens employed were designed such that the axial and torsional stresses might be assumed to be uniformly distributed over the cross section under a biaxial state of stress. Since the ratio of wall thickness to diameter was 0.027, thin wall torsion theory was applicable. The true variation in torsional stress across the wall was less than 3%, and the test length of the specimen great enough so that a uniform axial stress existed at the location of the strain gage.

The unit damping energy under the combined state of stress was determined by measuring the two stress-strain hysteresis loops which resulted when the specimen was cycled. The damping energy at a state of biaxial stress is considered to be the sum of the areas of the two principal stress-strain hysteresis loops, or

$$D(\sigma_1, \sigma_2) = \int \sigma_1 d\varepsilon_1 + \int \sigma_2 d\varepsilon_2 = D_1 + D_2,$$

where D_1, D_2 are the damping energies as measured from the σ_1-ε_1 and σ_2-ε_2 stress strain diagrams. Because of the changing in direction of the principal axes as the relative amounts of axial and torsional loads, α, are changed, the measurement of hysteresis loops in terms of the principal axes would require separate strain gages for each desired ratio of axial and torsional loading. As this would necessitate repeated relocations of strain gages on both specimen and dynamometer, a method of recording damping at any state of biaxial stress with one set of gages was developed. If the damping energy is dependent only upon the invariant features of the stress tensor, and the material isotropic, then the damping is also invariant with respect to a transformation of coordinates, and may be measured in any set of coordinates. Further, the damping energy may be measured by adding the damping energy observed by instrumentation designed to be sensitive to axial loading only to that observed by instrumentation designed to be sensitive to torsional loading only. The damping energy must be the equal of the net work done per cycle, and as the only work done is by the axial and torsional stresses, we find that the net work is given by

$$\int \sigma_a d\varepsilon_a + \int \sigma_s d\varepsilon_s = D_a + D_s,$$

where σ_a and σ_s are the stresses due to the axial and torsional loading, ε_a and ε_s are the strains as measured by axial strain gages (parallel and perpendicular to the axial loading) and torsional strain gages (gages aligned at 45% to the direction of axial loading), and D_a and D_s proportional to the areas of the respective hysteresis loops.

16

The areas of the axial and torsional hysteresis loops were measured with a planimeter and the damping associated with each loop was found from

$$D_a = K_a \lambda_a A_a \quad \text{and}$$

$$D_s = K_s \lambda_s A_s ,$$

where D_a and D_s are the net work inputs under combined loading, K_a and K_s are recorder calibration stress constants in psi/in. of deflection along the stress axis of the recorder; λ_a and λ_s are the strain constants in micro-inches/in of deflection along the strain axis of the recorder; A_a and A_s are the areas of the $\sigma_a - \varepsilon_a$ and $\sigma_s - \varepsilon_s$ hysteresis loops respectively, measured in square inches. The total damping energy of the material under the state of biaxial stress obtained from a combined axial and torsional loading is

$$D_T = D(\sigma_1, \sigma_2) = \int \sigma_a d\varepsilon_a + \int \sigma_s d\varepsilon_s .$$

V. RESULTS AND DISCUSSION

The data obtained experimentally is presented as plots of the unit damping energy versus the maximum principal stress for several values of α . Fig. 17, manganese copper and Fig. 18, Nivco 10, both display some amount of scatter, but are considered acceptable for purposes of observing the nature of behavior. From these figures, it is possible to ascertain the states of combined stress within the range of this investigation,

$$-1 \leq \alpha \leq 0 ,$$

which will produce equal amounts of unit damping. Such states of stress are indicated in Fig. 19 for the manganese copper alloy and as Fig. 20 for the magnetoelastic material, Nivco 10 alloy. In dimensionless form, these results appear as in Figs. 21 and 22 respectively. When plotted in this manner, the scatter in the data becomes much more apparent, however it may be seen that the effect of the lesser principal stress, σ_2 , is relatively small, suggesting that the combined stress damping for each material is dependent mainly on the magnitude of the greater principal stress. In terms of an equivalent stress theory, the maximum principal stress appears to be most appropriate.

These results do not seem to be easily reconciled with the theory advanced in section III, as the exponent n for both materials is seen from Figs. 17 and 18 to be less than three, and an examination of Fig. 6 reveals that none of the critical stresses there

17

considered will produce such behavior. Consequently, either the validity of this theory in general, or its application to these materials must be questioned.

Cochardt (12), in a discussion of the damping of a magneto-elastic material, a 12% chrome steel turbine blade material, shows that the maximum energy loss due to magnetoelastic damping in a state of torsional stress should be the same as the maximum energy loss in a state of tension. He assumed, since it was considered impossible to determine the exact relationship, that the torsional stress necessary to produce this maximum damping would be one half of the tensile stress. This leads directly to the conclusion that a state of torsional stress will produce the same damping as a state of tensile stress of twice the magnitude. No previous attempts at the prediction of biaxial stress damping properties for manganese copper are known of at the present time.

If one considers the influence of residual stress on the damping of each of these materials, it becomes apparent that for residual stress other than hydrostatic, these materials are highly anisotropic in their damping behavior, and consequently, it would appear that no simple (isotropic) theory may be expected to give a reasonable prediction of their combined stress damping behaviors. It is also to be anticipated that these materials would display quite different behavior, both quantitatively and qualitatively, if the specimen orientation with respect to rolling direction were to be changed. It is to be noted in Fig. 18 that the slope of the damping stress relationship is considerably less than the value of three which is to be expected of a material whose dominant damping mechanism is magnetoelastic. It thus appears that the Nivco 10 specimens used in this investigation were not behaving as a magnetoelastic material, likely a result of removing the residual stresses necessary for the magnetoelastic behavior (13) by the machining operations. This possibility was investigated. The specimens blanks were found to have a BHN of about 300 in the as-received condition (properly heat treated for high damping). The test section of a prepared specimen was subjected to a hardness test, and the BHN found to be about 100. Cochardt has published (13) a curve of damping vs. hardness for a material of quite similar composition. His results indicate a very sharp dropping off of damping as hardness is permitted to vary in either direction from the value corresponding to optimum damping. Thus, we might expect that at the observed lower values of hardness, the magnetoelastic damping mechanism is not strictly dominant, but rather that the damping is due to a combination of the magnetoelastic phenomenon and other mechanisms quite likely local plastic deformations.

18

VI.   SUMMARY AND CONCLUSIONS

In the past, the usual procedure employed for the description and prediction of combined stress damping properties was the equivalent stress approach. This means was employed by Yorgiadis and Anderson, and somewhat indirectly by Whittier, but has not proved to be entirely satisfactory.

A new theory was developed incorporating one of the most significant features of material damping, i.e., the dependence of damping on a nth power of the applied stress. This nth power law as observed for uniaxial stress was extended to states of biaxial stress through several assumptions, notably:

1.   that the material is isotropic;

2.   that the same mechanism of damping is operative at all states and magnitudes of stress;

3.   that the shape of the hysteresis loop is the same at all states of stress (This may well be related to 2.); and

4.   that the effects of such variables as temperature, frequency and stress history will be the same at all states of stress (This should be a consequence of 2, as the nature of these effects depends on the operative mechanism).

This new theory predicts biaxial stress damping properties to within a multiplicative function of the state of stress. This function is somewhat arbitrary. It may either be selected on the basis of experimental results for the material in question or chosen to be the same as in a similar material for which the proper function already is known.

The results of a previous investigation by V. W. Anderson are satisfactorily described by the new theory. Tests were conducted on two newer materials, Nivco 10 and manganese copper, but in these cases the new theory does not give a satisfactory description of the biaxial stress damping properties. A much stronger dependence on the greater principal stress was observed in these materials than is predicted. One essential difference exists between the testing procedures for the two groups of materials and should be considered. It was considered desirable to perform tests at moderate stress levels in order to avoid the difficulty in obtaining reproducible data which is experienced when stress history effects are present. Readily measurable damping was obtained at stress levels below σ_c in the case of the high damping alloys Nivco 10 and manganese copper, but it was found necessary to test the copper and steel at relatively higher levels of stress (above their sensitive limits, σ_c) in order to obtain measurable damping.

19

This difference may be of some significance in any comparison of results for the two groups of materials. It is also suspected that these high damping materials may display strong directional properties which were not investigated.

Of a greater significance, however, is the mechanism of damping operative in each case. It is to be noted that the materials for which the new theory gives satisfactory agreement are materials which dissipate energy by means of local plastic deformations, whereas other mechanisms are normally dominant in the two materials for which the theoretical predictions are inadequate. As a consequence of this, the new theory should at least be limited in application to materials for which the dominant damping mechanism is that of plastic deformations. Since even the uniaxial damping characteristics of two materials of different mechanisms are quite dissimilar, it is probable that no theory of combined stress damping can be formulated that will be valid for all mechanisms. It is likely that a separate theory will be necessary for each mechanism of interest.

Further experimental investigation would be desirable. In addition to the testing of materials displaying different mechanisms under combined axial and torsional loadings, data obtained from other states of biaxial stress would be useful. For instance, the providing of internal pressures in suitable combinations with axial loads would greatly increase the portion of the σ_1-σ_2 diagram which might be reached experimentally. The measurement of damping energy under a cyclic hydrostatic pressure would be very interesting, although experimentally difficult.

20

VII. LIST OF REFERENCES

1. Lazan, B. J., "Energy Dissipation Mechanisms in Structures, with Particular Reference to Material Damping," Structural Damping, Papers presented at a Colloquium on structural damping held at the ASME annual meeting in Atlantic City, N. J. in December 1959.

2. Lazan, B. J., "Damping and Resonant Fatigue Behavior of Materials," Proc. of the Int. Cong. of the Fatigue of Metals, London, Sept. 1956.

3. Demer, L. J., "Bibliography of the Material Damping Field," WADC Technical Report 56-180, June 1, 1956.

4. Robertson, J. M. and Yorgiadis, A. J., "Internal Friction in Engineering Materials," J.A.M., Sept. 1946, pp. A-173-182.

5. Anderson, V. W., "Damping Properties of Materials Subjected to Various Ratios of Biaxial Stress," Ph.D. thesis, University of Minnesota, April 1960.

6. Whittier, J. S., "Phenomenological Theories of Hysteretic Material Damping with Application to the Vibration of Circular Plates," A.S.D. Tech. Rep. 61-264, University of Minnesota, June 1961.

7. Marin, J., Engineering Materials, Prentice-Hall, New York, 1952, pp. 198-210.

8. Lazan, B. J., "A Study with New Equipment of the Effects of Fatigue Stress on the Damping Capacity and Elasticity of Mild Steel," Trans. A.S.M., Vol. 4, pp. 499-558 (1950).

9. Demer, L. J. and Lazan, B. J., "The Effect of Stress Magnitude and Stress History on the Damping, Elasticity, and Fatigue Properties of Metallic Materials," Dept. of Mechanics and Materials, University of Minnesota, under sponsorship of the ONR, U. S. Navy, Contract N8-ONR 66207, Project Nr-064-361, Sept. 1953.

10. Torvik, P. J., "Damping Properties of a Cast Magnesium and a Manganese Copper Alloy Proposed as a High Damping Material," Appendix 72 f.g., Status Report 58-4 by B. J. Lazan, University of Minnesota, Dec. 31, 1958.

11. Lazan, B. J. and Wu, T., "Damping, Fatigue and Dynamic Stress Strain Properties of Mild Steel," Proc. ASTM, Vol. 51, pp. 649-681 (1951).

12. Cochardt, A. W., "The Origin of Damping in High Strength
    Ferromagnetic Alloys," J.A.M., June 1953, Vol. 20, No. 2, pp.
    196-200.

13. Cochardt, A. W., "Development of a Ferromagnetic Cobalt Base
    High Temperature Alloy," Trans. ASM, Vol. 52, 1960, pp. 914-928.
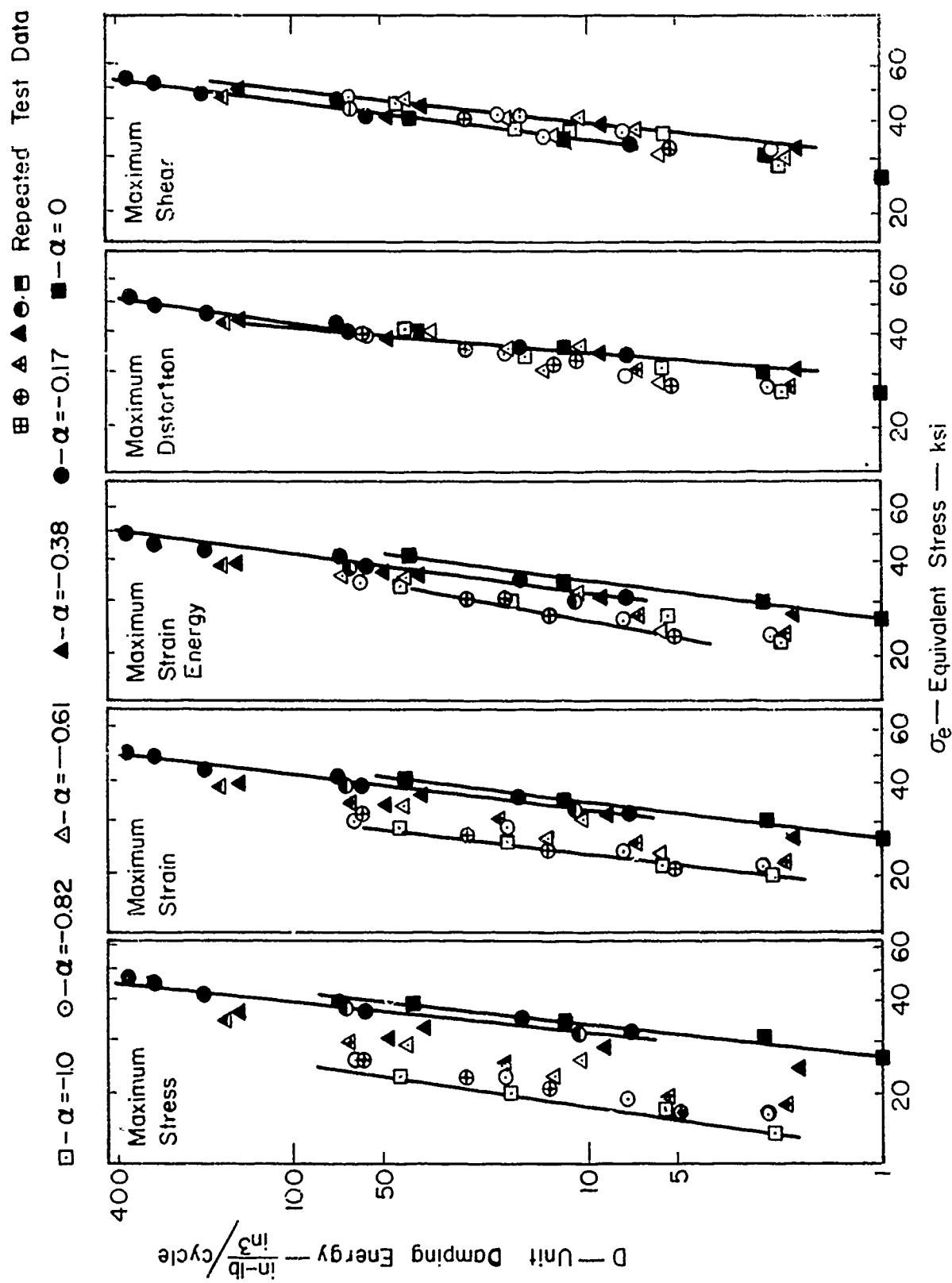
Fig. 1   Unit Damping Energy of 1020 Steel as a Function of Equivalent
Stress for Various Principal Stress Ratios, α (Data Due to Anderson)

23
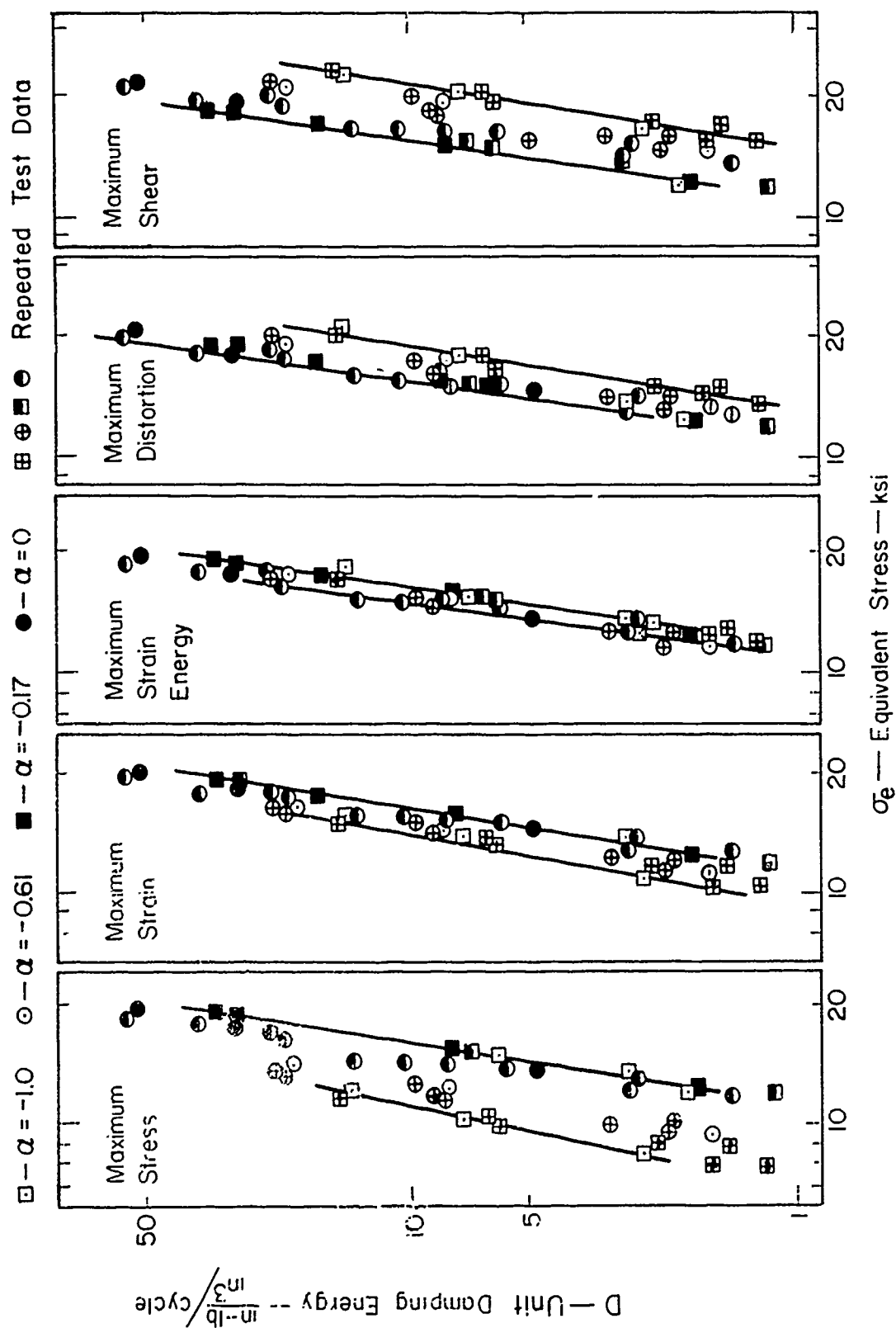
Fig. 2   Unit Damping Energy of Pure Copper as a Function of Equivalent Stress for Various Principle Stress Ratios, α (Data Due to Anderson)

24
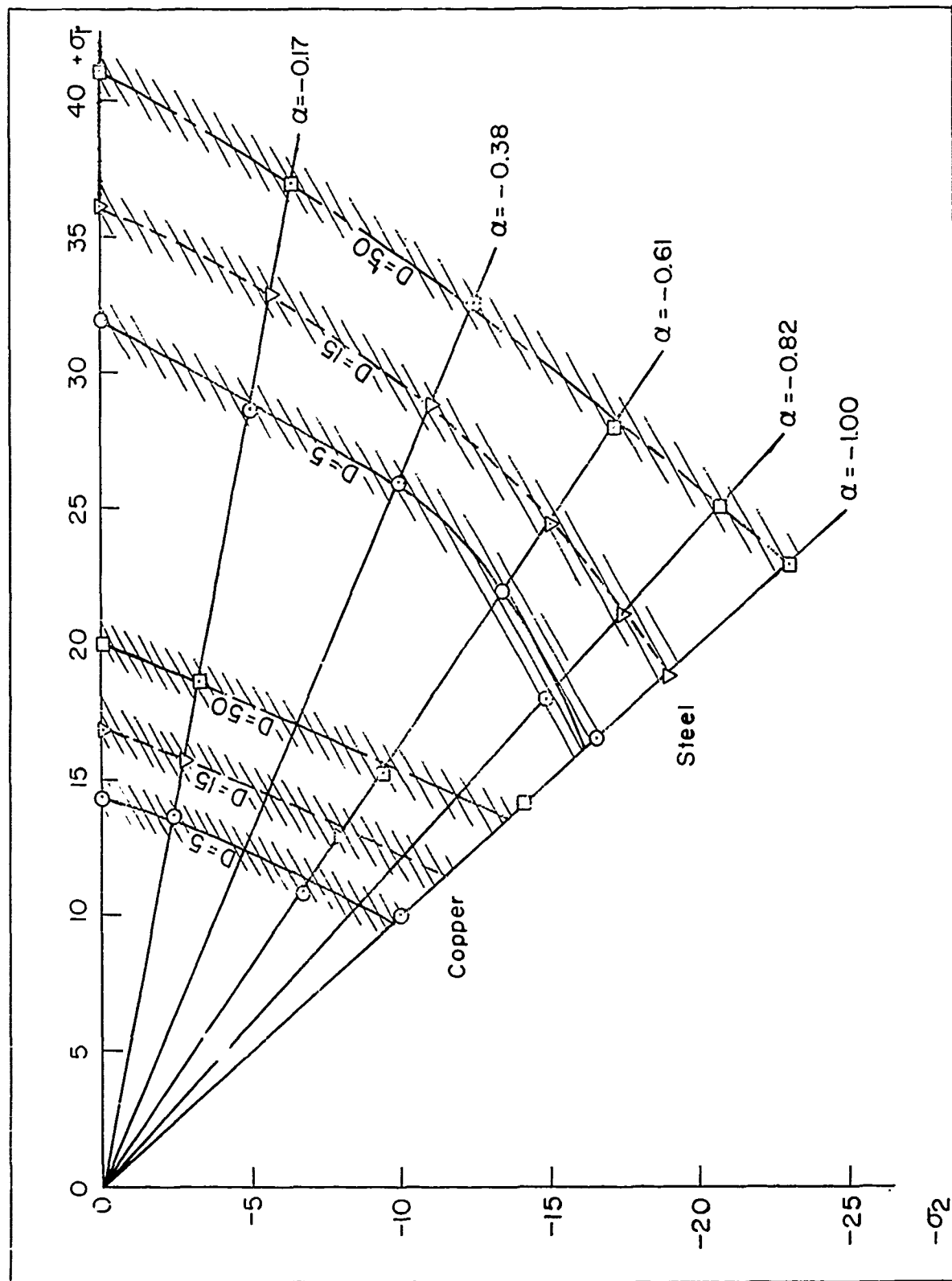
Fig. 3 $\sigma_1 - \sigma_2$ Diagram Showing Lines of Iso-Damping for IO2O Steel (Data Due to Anderson) and Pure Copper

25
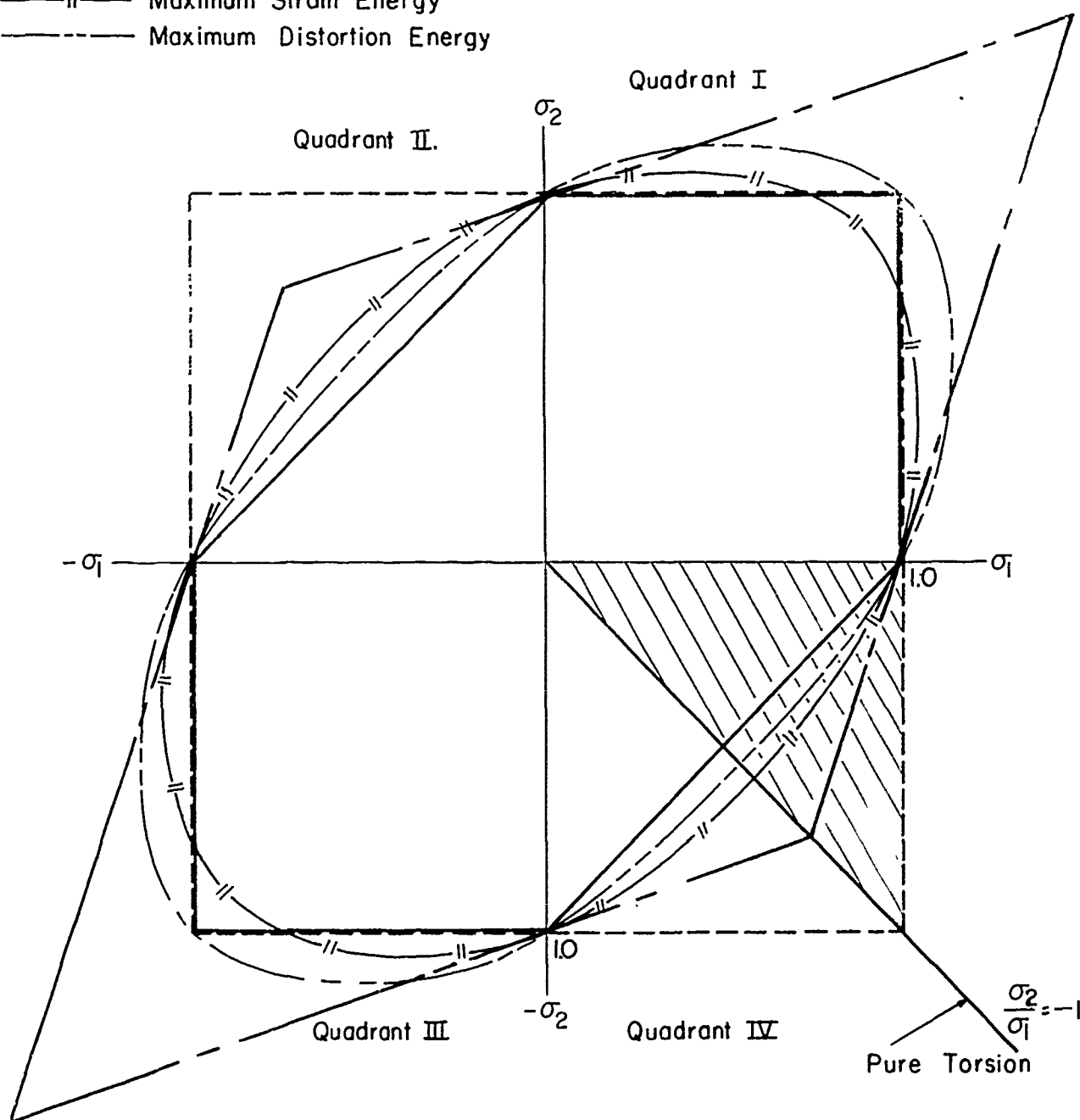
Fig. 4   Diagram Showing Various Theories of Combined Stress in Terms of Principal Stresses

26
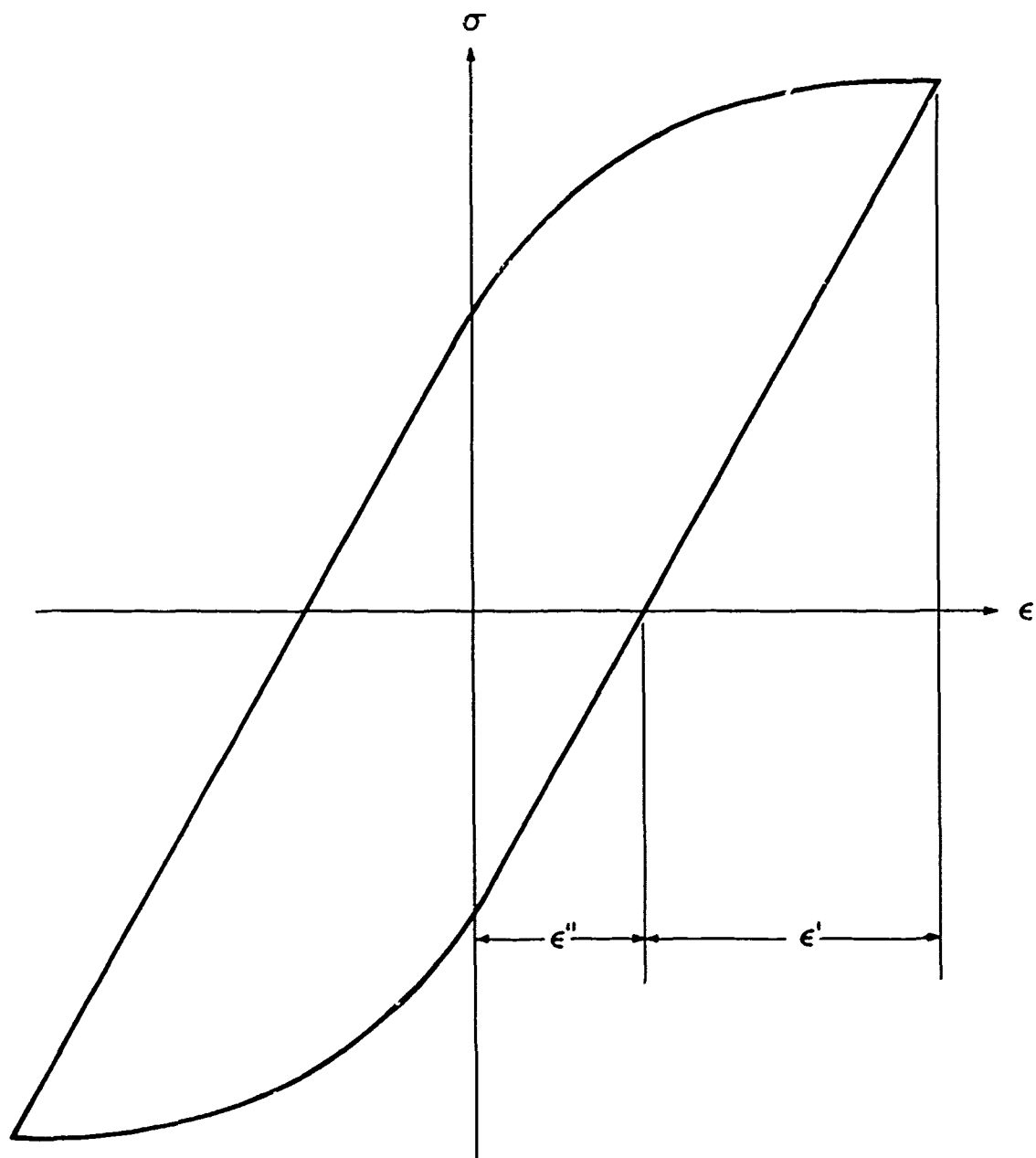
Fig. 5   Typical Hysteresis Loop for a   Metallic   Material

27
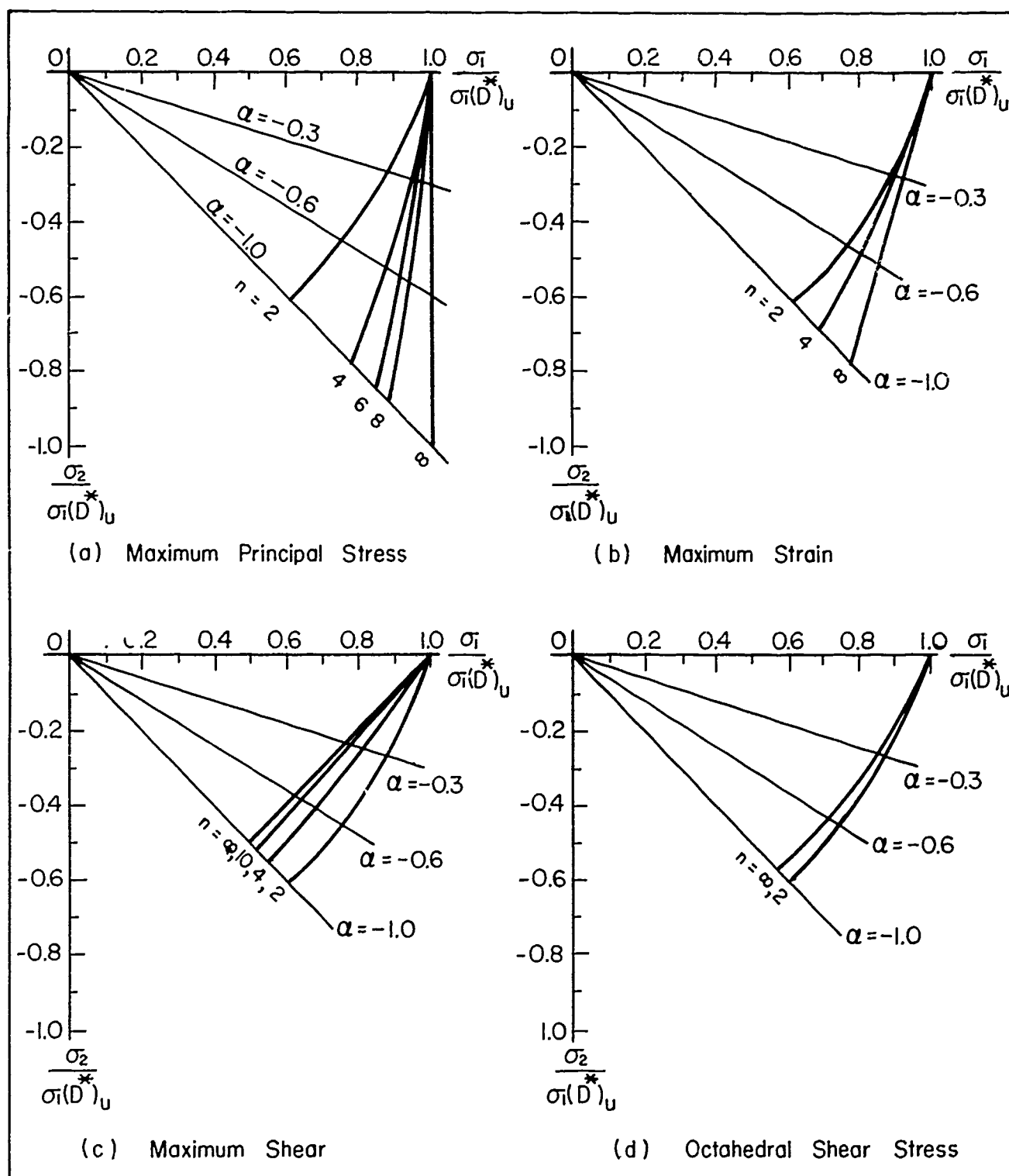
Fig. 6   Dimensionless   Iso-Damping   Lines   (Theoretical)   for   Various Significant   Stresses

28
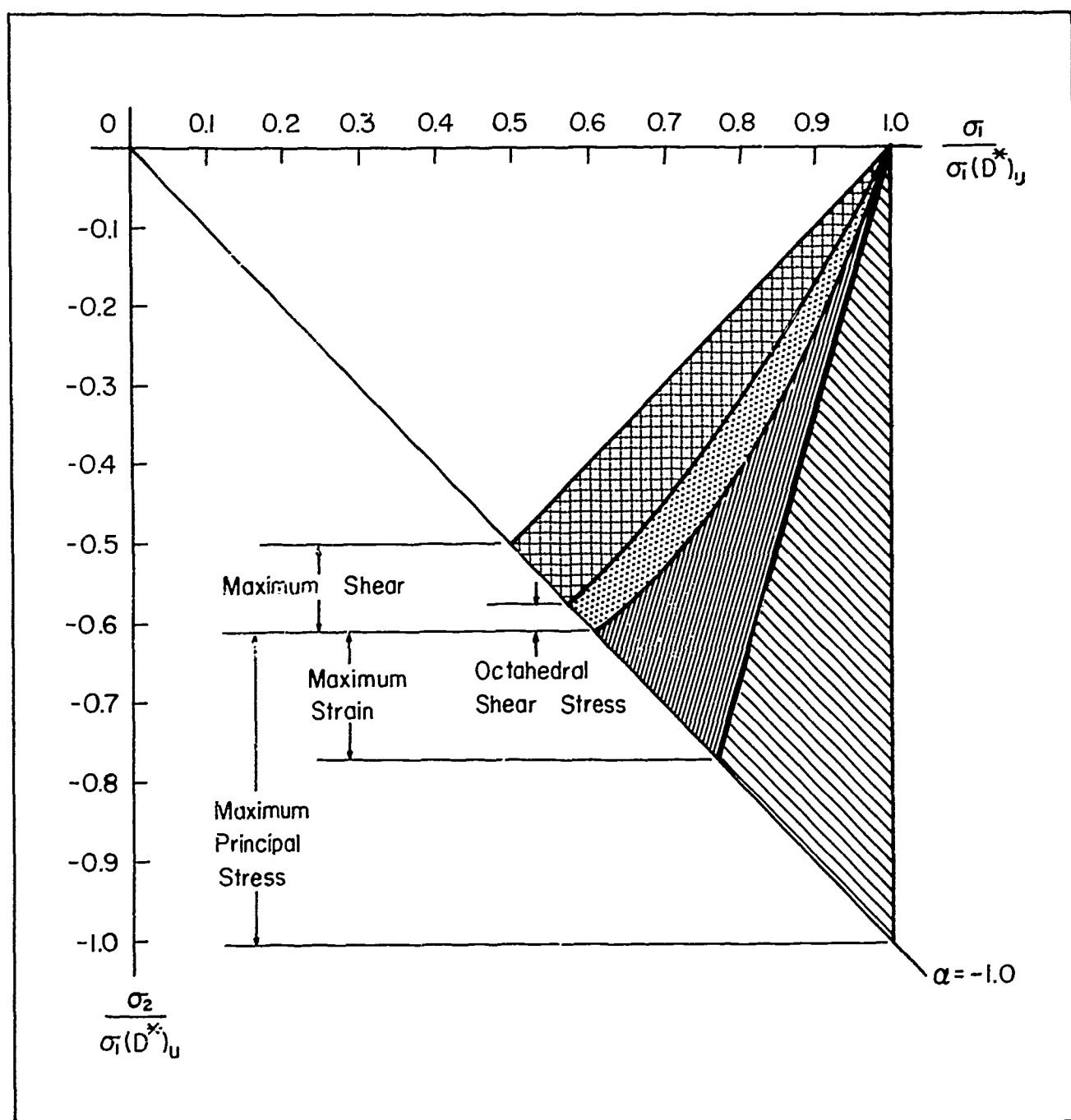
Fig. 7   Possible   Location   of   Iso-Damping   Lines   for   Various
           Significant   Stresses

29
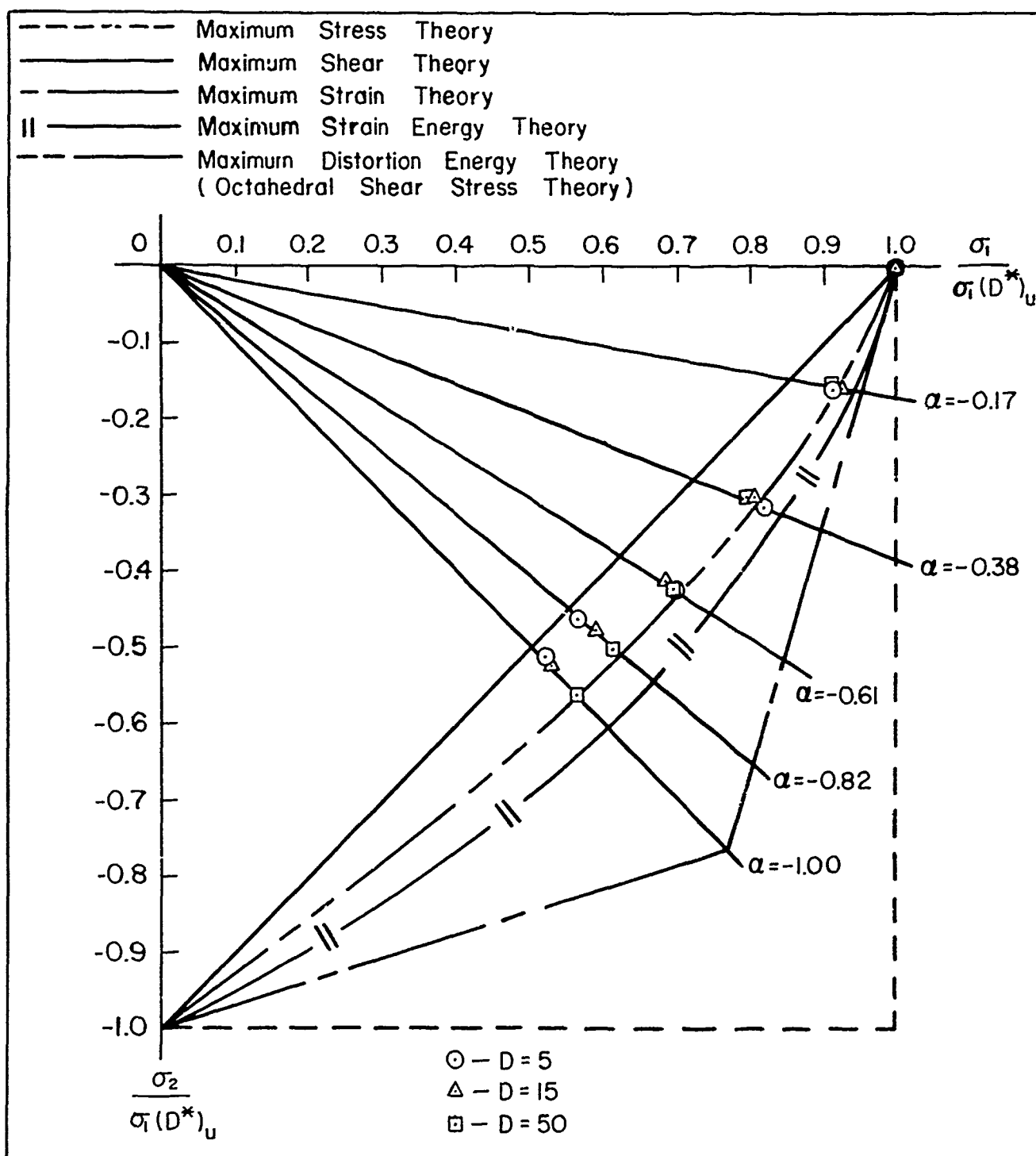
Fig. 8 $\sigma_1 - \sigma_2$ Diagram Showing Theories of Combined Stress Applicable to Damping Properties of SAE 1020 Steel under Reversed Stress   (Data Due to Anderson)
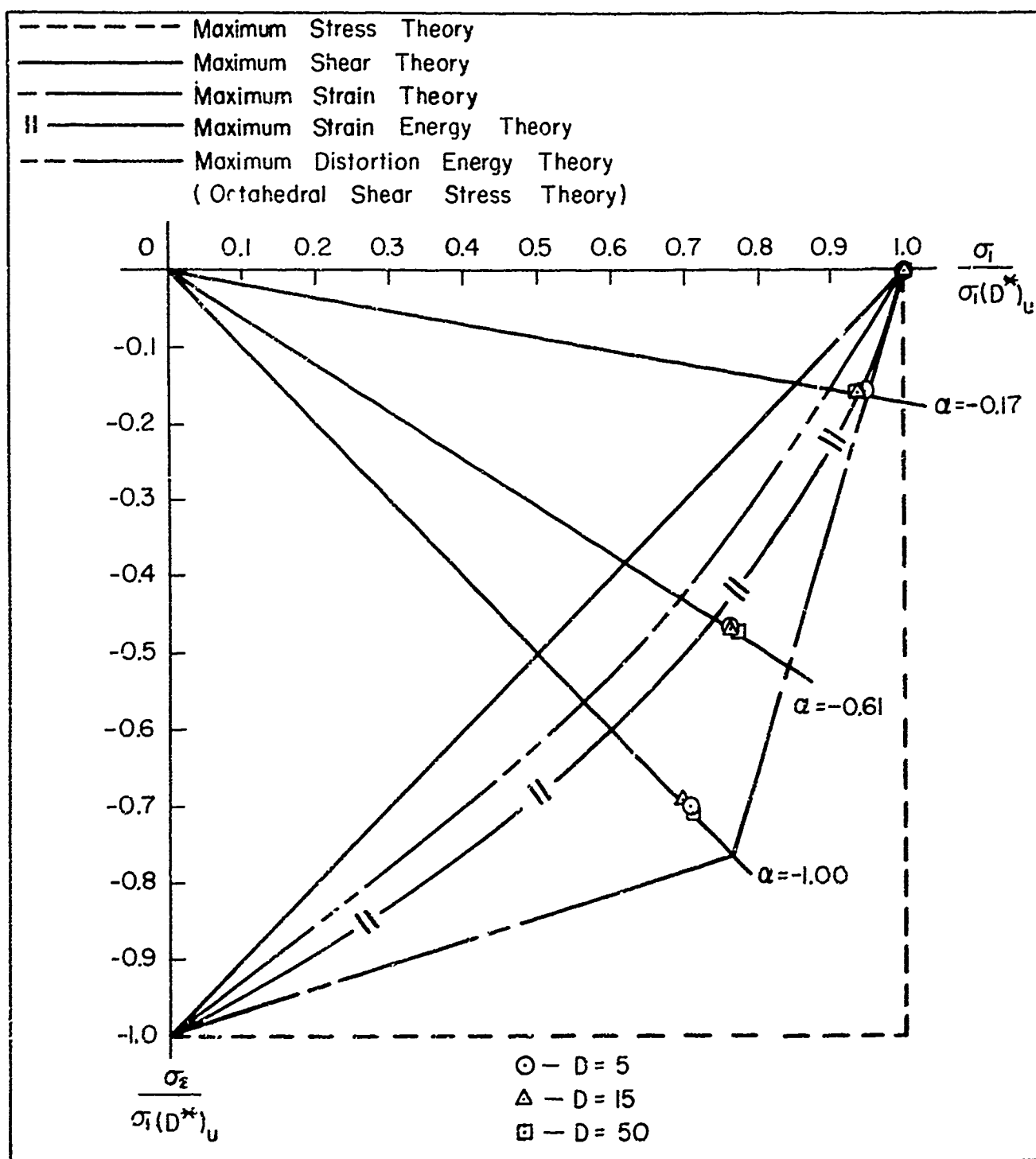
Fig. 9 $\sigma_1 - \sigma_2$ Diagram Showing Theories of Combined Stress
Applicable to Damping Properties of Pure Copper
under Reversed Stress   (Data Due to Anderson)

31
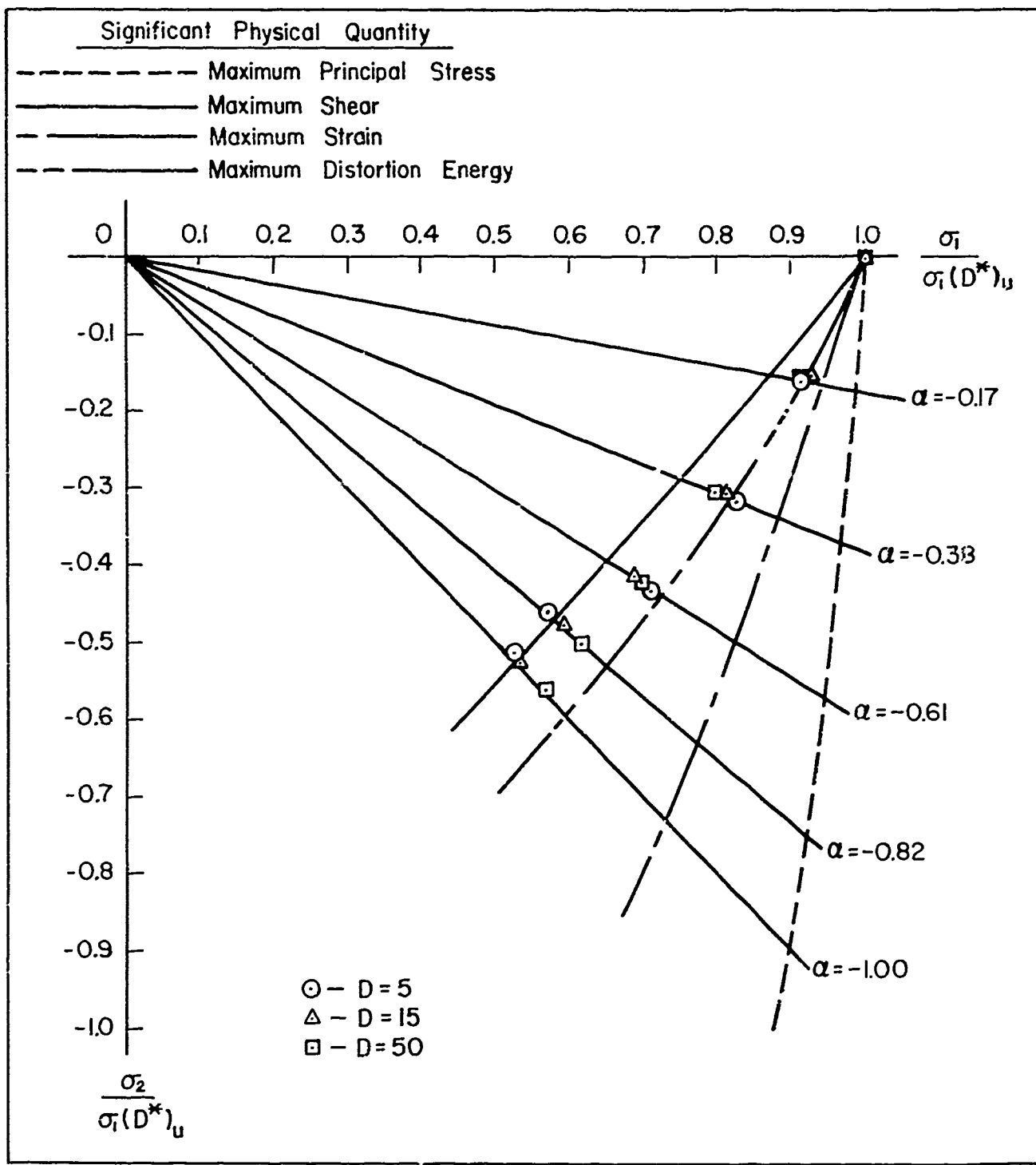
Fig. 10   Comparison of Experimental Values for Mild Steel with Theoretical Iso-Damping Lines for Various Significant Stresses (n = 11)   (Data Due to Anderson)
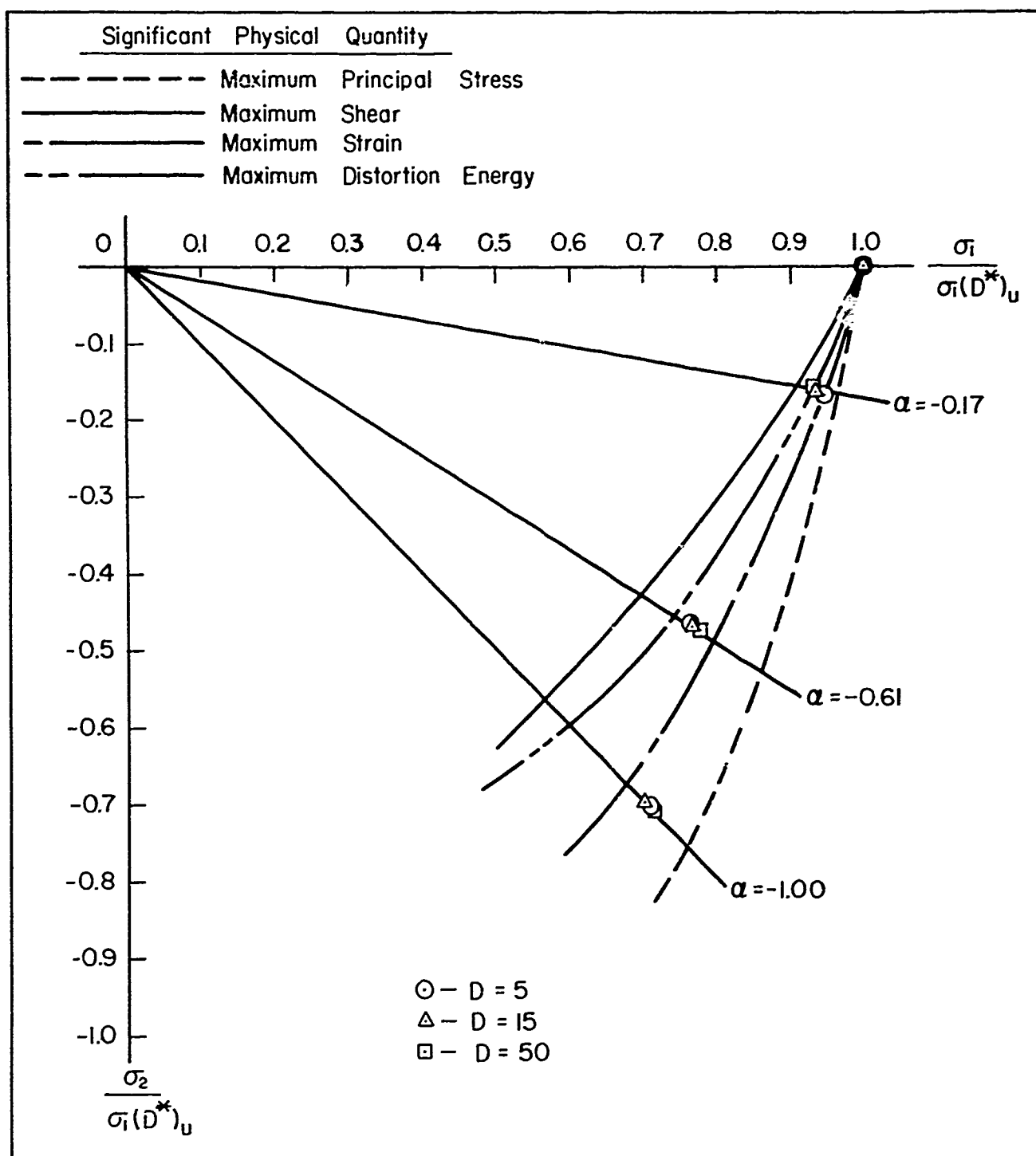
Fig. 11   Comparison of Experimental Values for Pure Copper with Theoretical Iso-Damping Lines for Various Significant Stresses ($n = 3.5$)   (Data Due to Anderson)

33
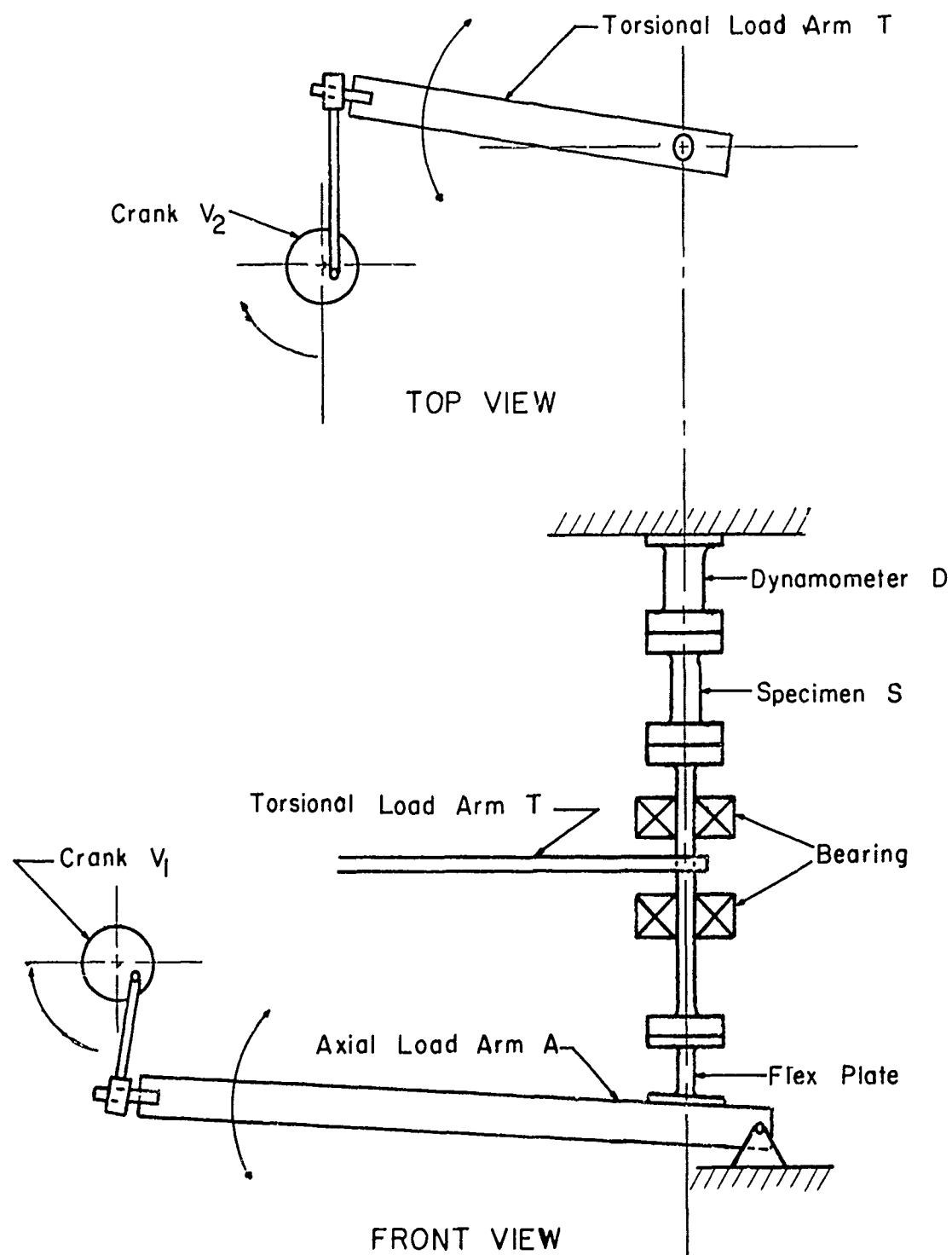
Fig. 12　Schematic　Diagram　of　Biaxial　Stress　Damping　Machine

34
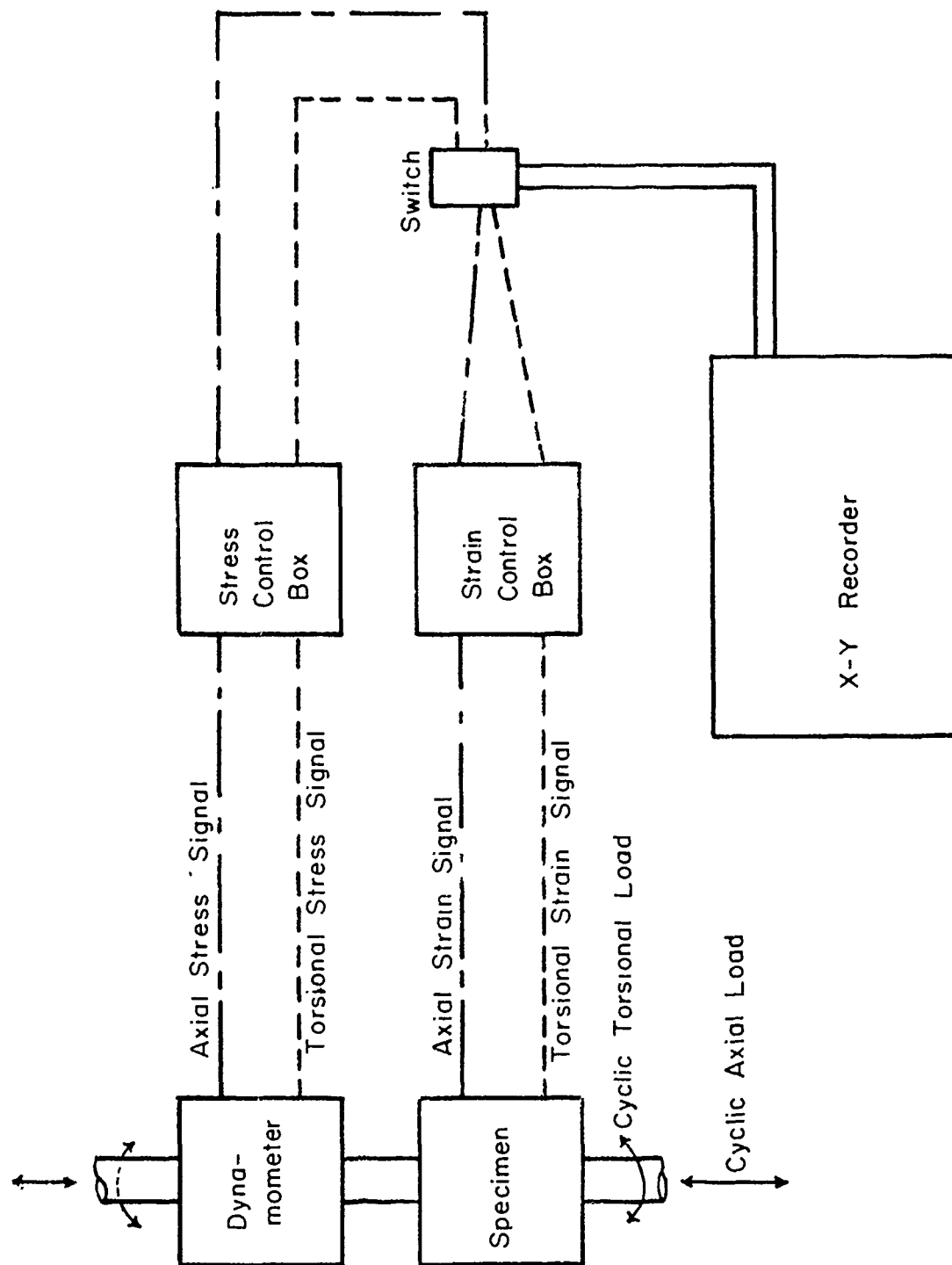
Fig. 13   Block Diagram of the Instrumentation of the Experimental Set-up

35
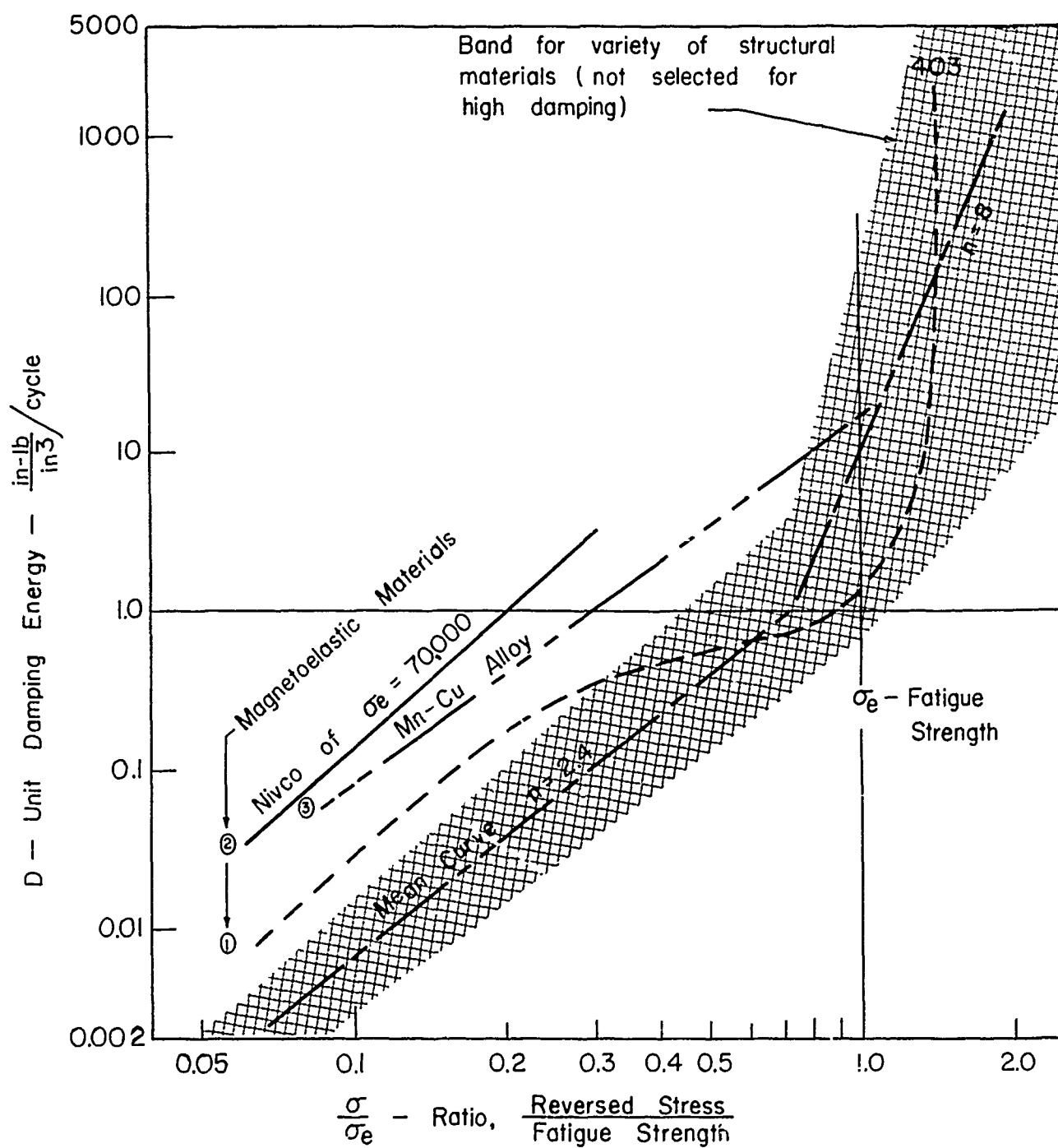
Fig. 14   Unit Damping Energy of Various Structural Materials

36

Fig. 15   Type ND Biaxial Stress Damping Specimen

37
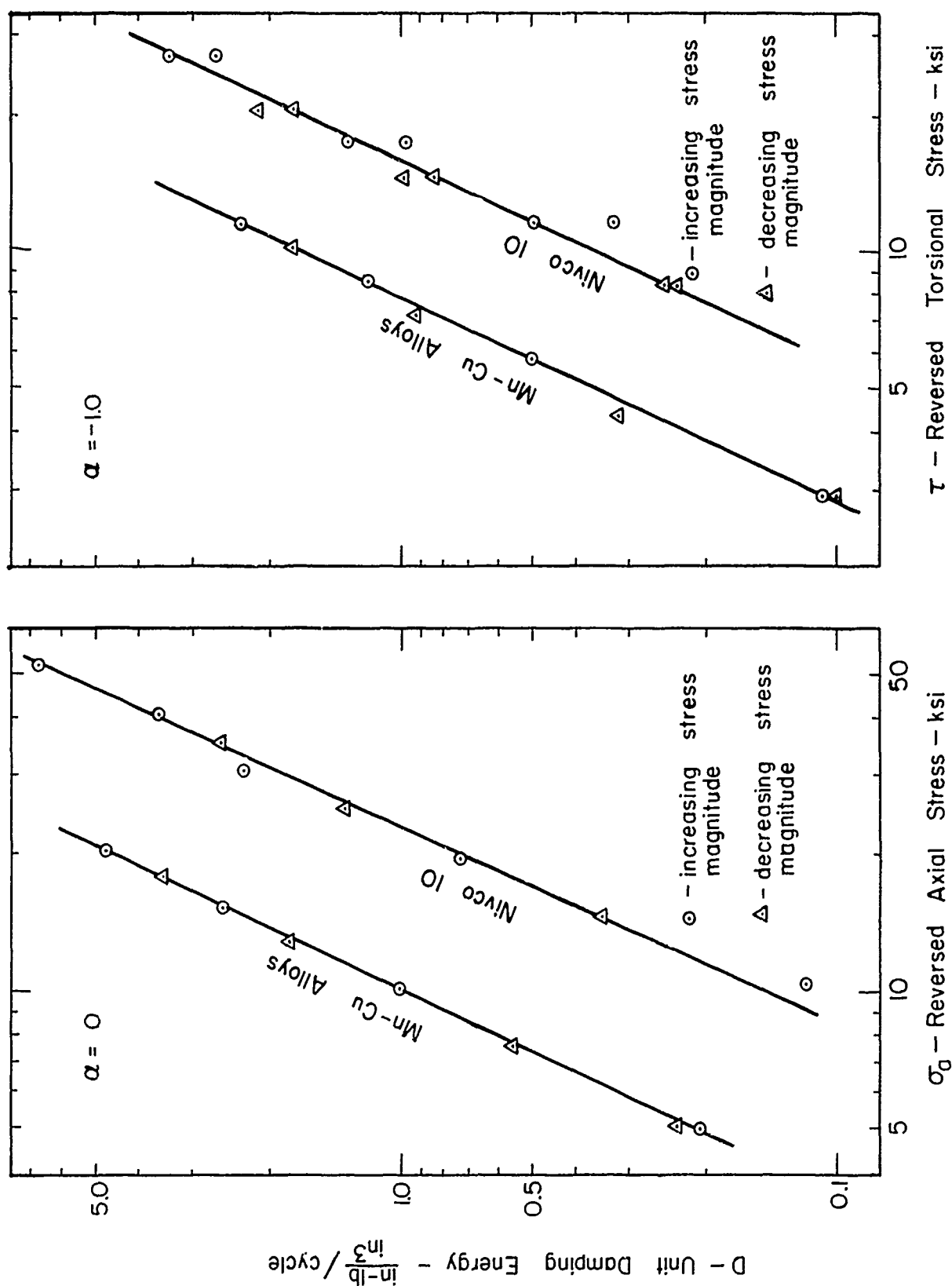
Fig. 16   Effect of Stress History on the Unit Damping Energy of Mn–Cu Alloys and Nivco 10 as a Function of Reversed Stress
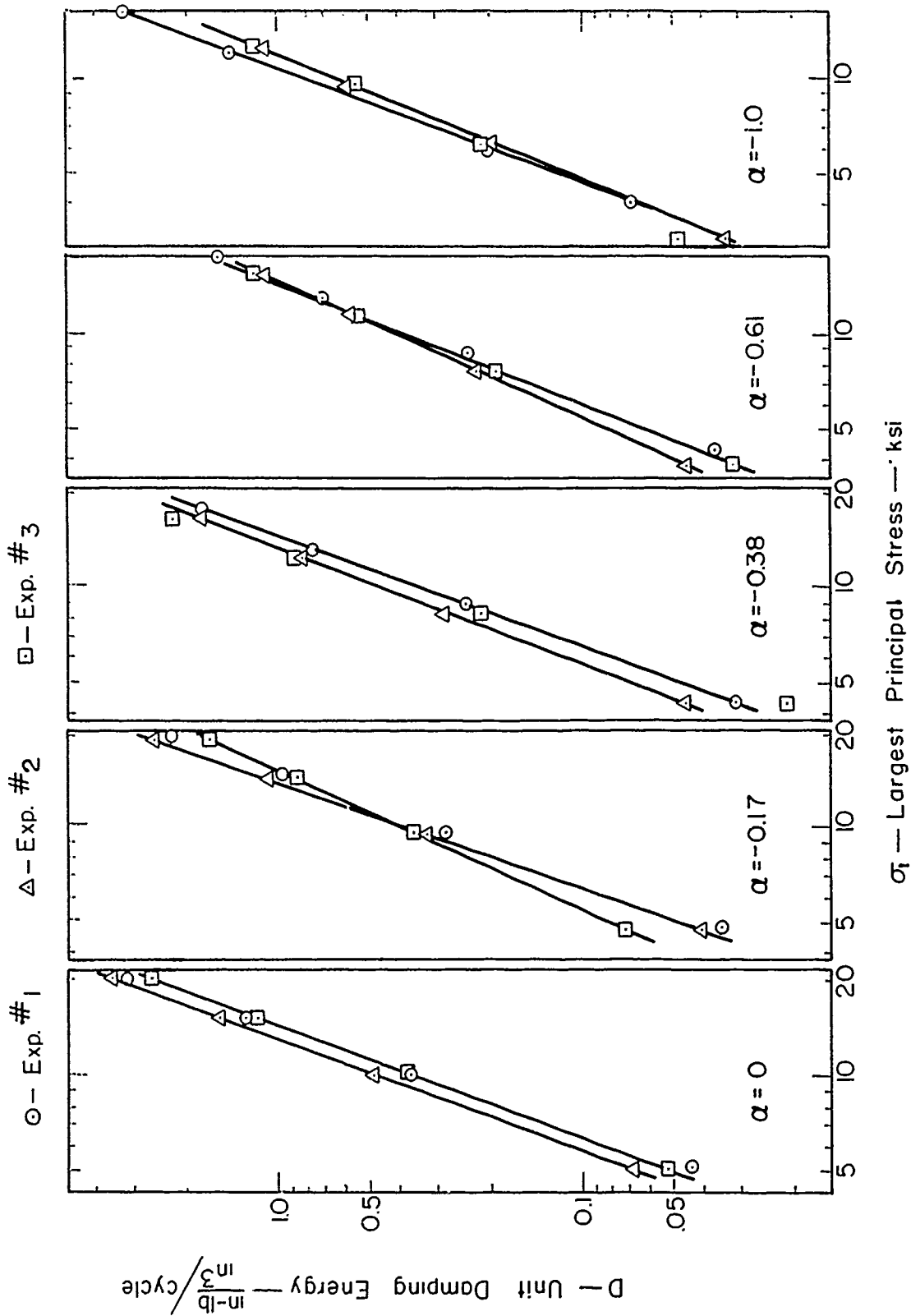
Fig. 17 Unit Damping Energy of Manganese Copper (CDC #780) Alloy as a Function of Principal Stress, σ_1 for Various Principal Stress Ratios, α

σ_1 — Largest Principal Stress — ksi

D — Unit Damping Energy — $\frac{\text{in-lb}}{\text{in}^3/\text{cycle}}$

$\odot$ — Exp. #1

$\triangle$ — Exp. #2

$\square$ — Exp. #3

$\alpha = 0$

$\alpha = -0.17$

$\alpha = -0.38$

$\alpha = -0.61$

$\alpha = -1.0$
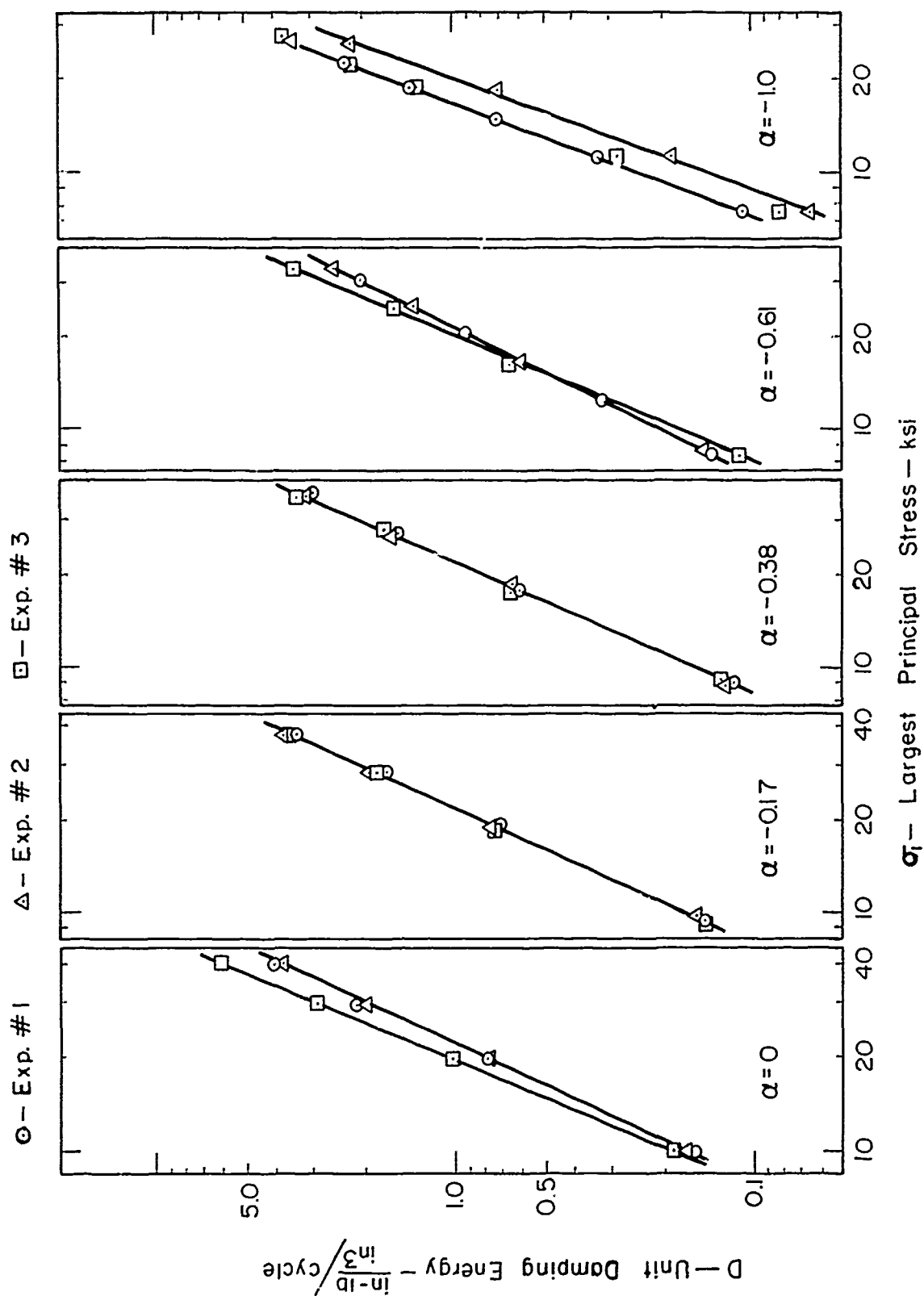
Fig. 18   Unit Damping Energy of Nivco 10 Alloy as a Function of Principal Stress, σ_i for Various Principal Stress Ratios, α

40
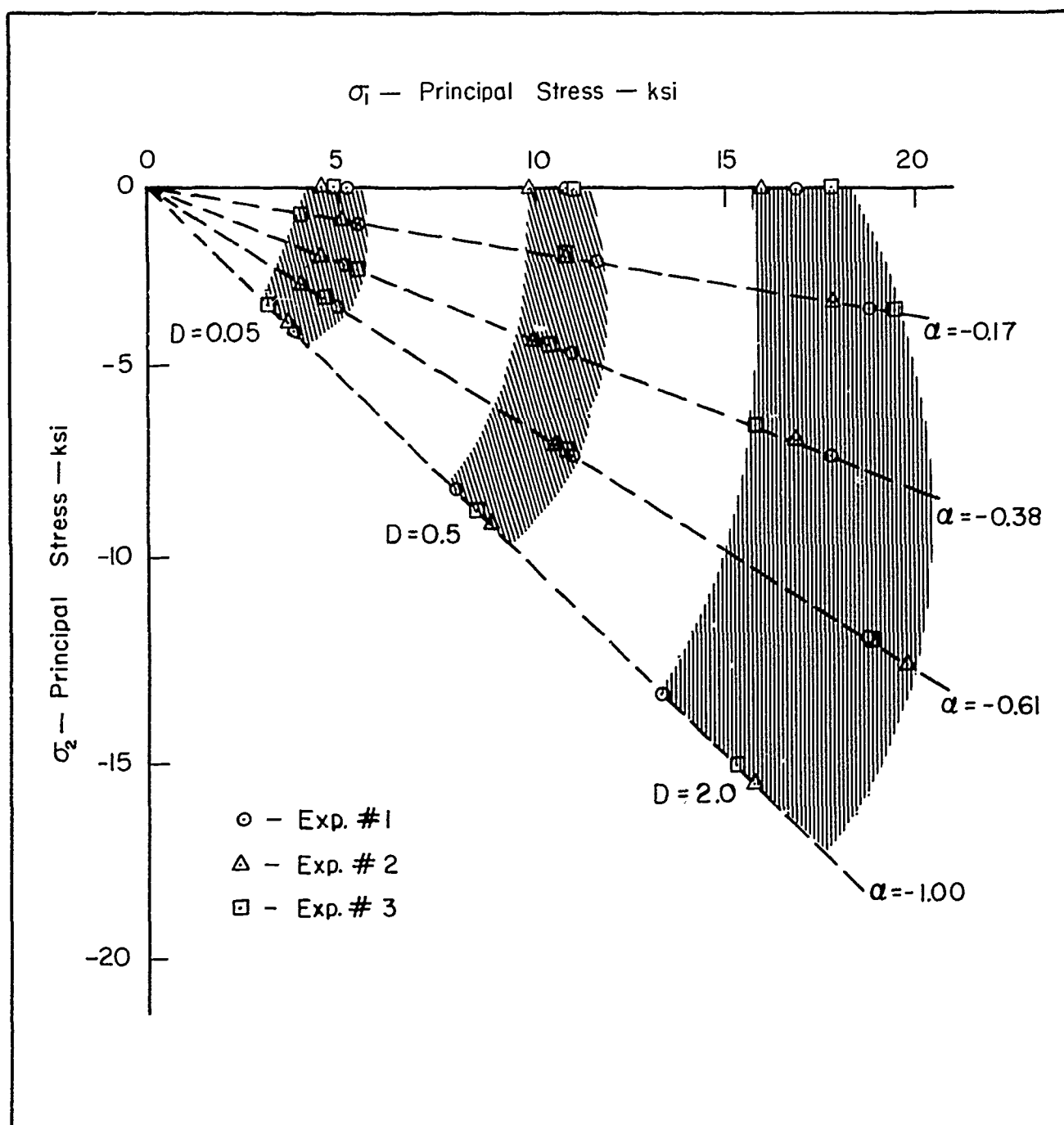
Fig. 19 $\sigma_1 - \sigma_2$ Diagram Showing Points of Iso-Damping for Manganese – Copper (CDC # 780) Alloy
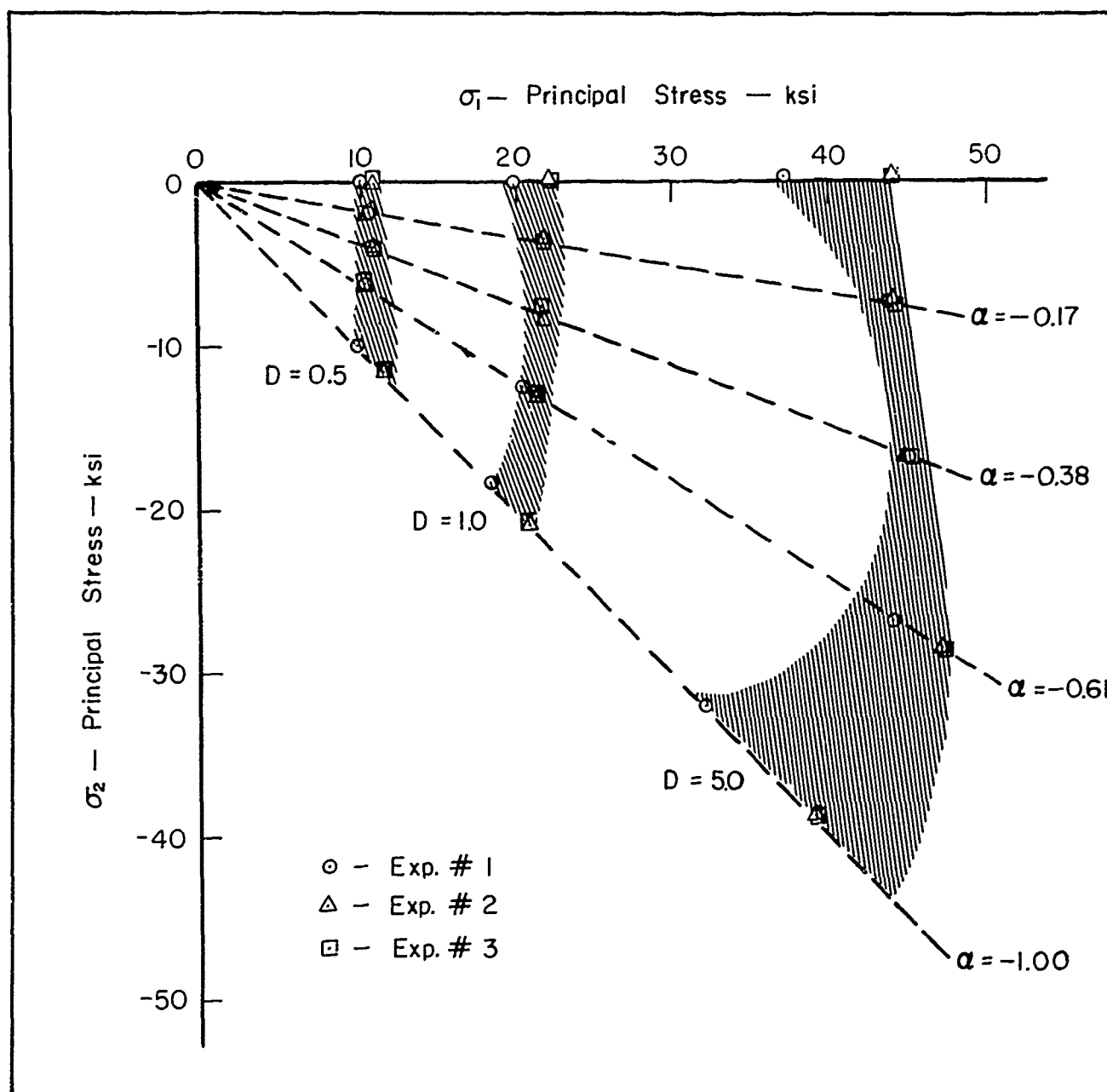
Fig. 20 $\sigma_1 - \sigma_2$ Diagram Showing Points of Iso-Damping for
          Nivco 10 Alloy

42
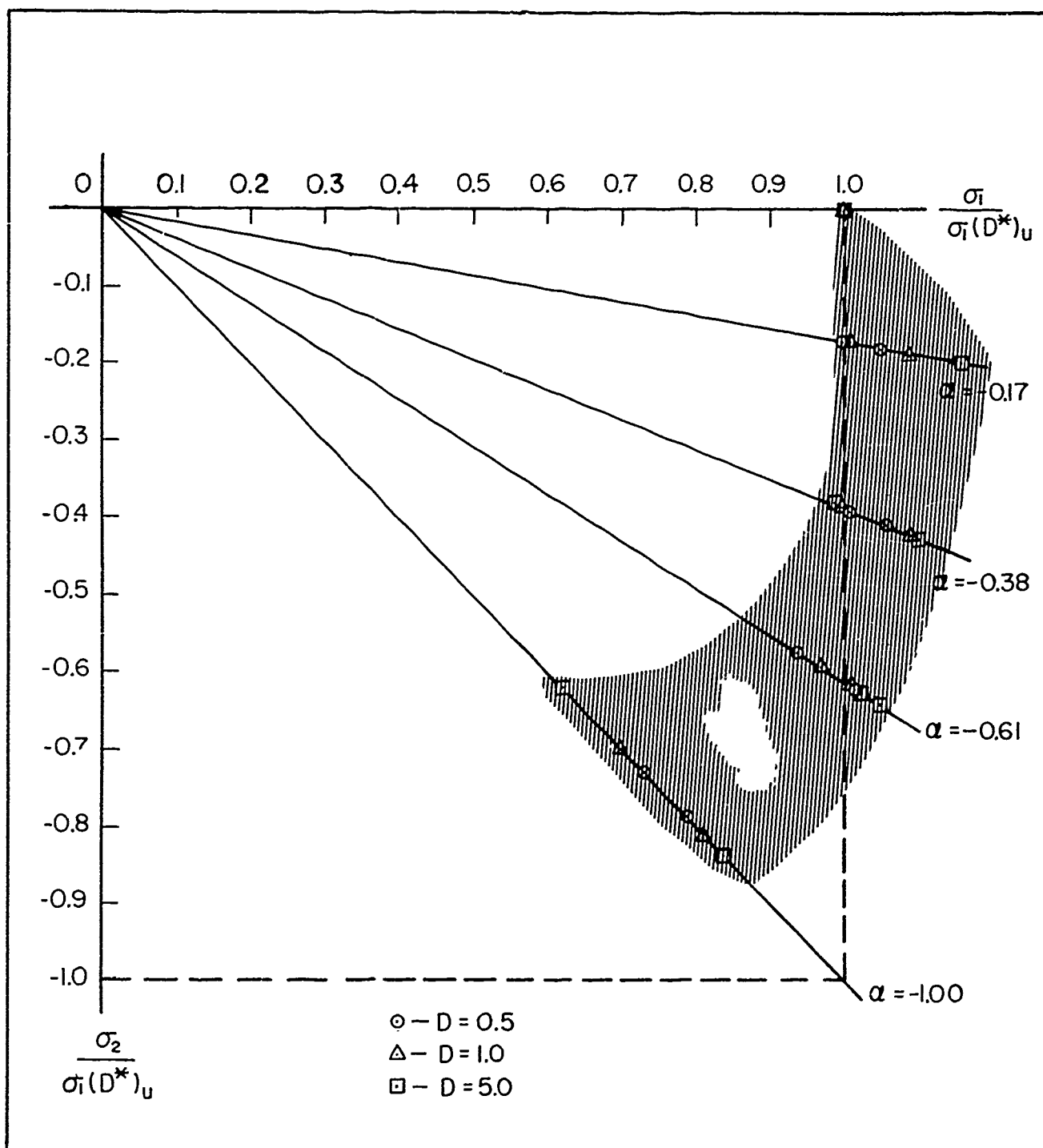
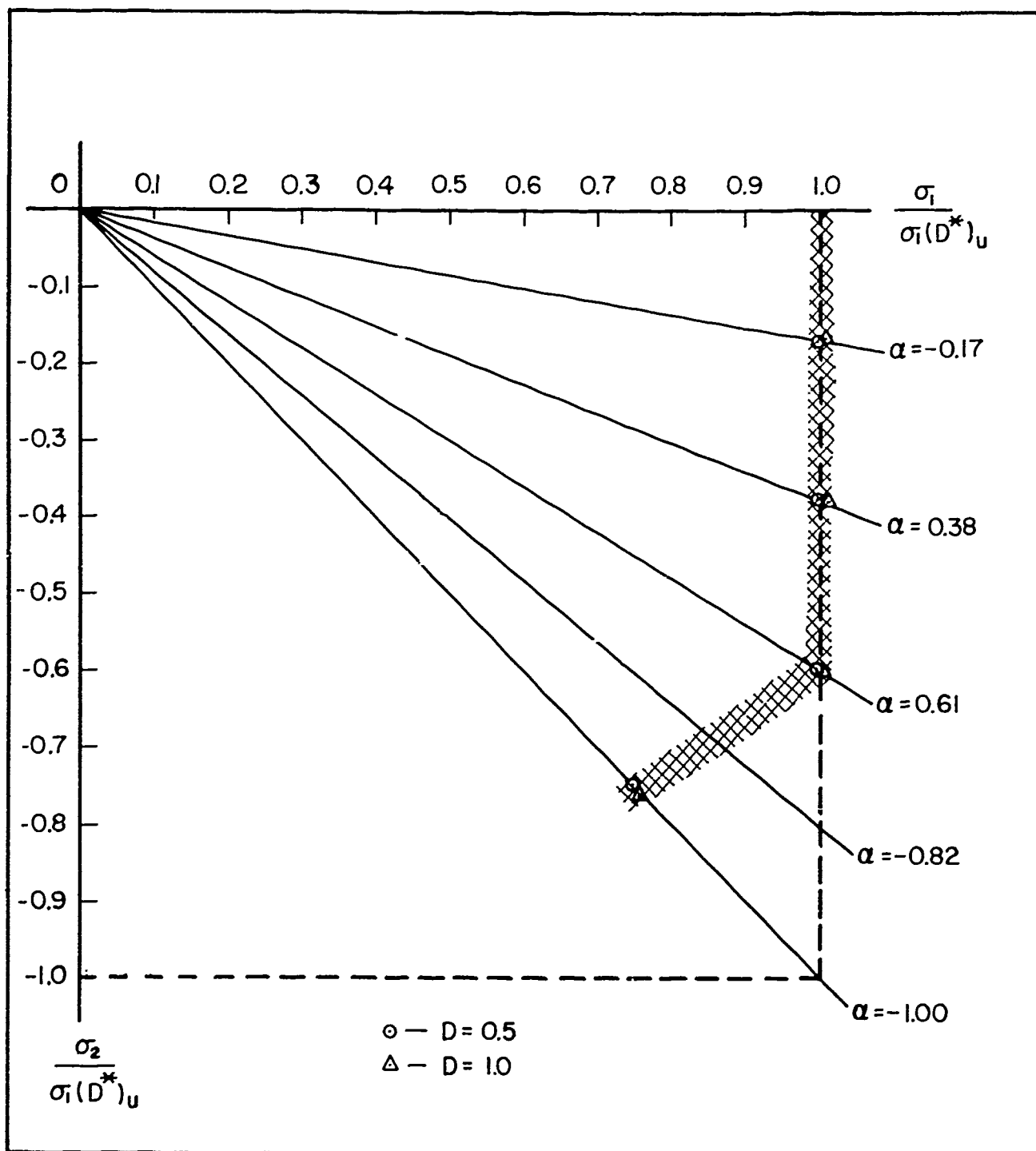Fig. 21   Locus of Experimentally Determined Iso-Damping Lines
           for Manganese Copper Alloy

43

Fig. 22   Locus of Experimentally Det .rmined Iso– Damping Lines
for Nivco IO Alloy

44

TABLE 1

Critical Physical Quantity	$\sigma_*(\sigma_1, \sigma_2)$	$\Gamma(\sigma_1, \sigma_2)$	$D(\sigma_1, \sigma_2)$
1. Maximum Stress	σ_1	$\dfrac{EJ}{K}\sigma_1^{n-2}$	$J\sigma_1^n(1-2\nu\alpha+\alpha^2)$
2. Maximum Strain	$\sigma_1 - \nu\sigma_2$	$\dfrac{EJ}{K}\sigma_1^{n-2}(1-\nu\alpha)^{n-2}$	$J\sigma_1^n(1-2\nu\alpha+\alpha^2)(1-\nu\alpha)^{n-2}$
3. Maximum Shear	$\sigma_1 - \sigma_2$	$\dfrac{EJ}{K}\sigma_1^{n-2}(1-\alpha)^{n-2}$	$J\sigma_1^n(1-2\nu\alpha+\alpha^2)(1-\alpha)^{n-2}$
4. Maximum Octahedral Shear Stress	$\sqrt{\sigma_1^2 - \sigma_1\sigma_2 + \sigma_2^2}$	$\dfrac{EJ}{K}\sigma_1^{n-2}(1-\alpha+\alpha^2)^{\frac{n-2}{2}}$	$J\sigma_1^n(1-2\nu\alpha+\alpha^2)(1-\alpha+\alpha^2)^{\frac{n-2}{2}}$

Aeronautical Systems Division, Dir/Materials and Processes, Metals and Ceramics Lab. Wright-Patterson AFB, Ohio. Rpt Nr ASD-TDR-62-1030 DAMPING OF MATERIALS UNDER BIAXIAL STRESS. Summary report, May 62, 45 p. incl. illus., tables, 13 refs.

Unclassified report

A new theory of combined stress damping is developed and evaluated on the basis of experimental results for several materials. It is concluded that the new theory should be limited in application to materials whose dominant damping mechanism is known to be plastic deformation. It appears that a
(over)

separate theory of combined stress damping may be required for each mechanism of damping.

1. Mechanical Properties
2. Damping
I. AFSC Project 7351, Task 735106
II. Contract AF 33 (657)-7453
III. University of Minnesota, Minneapolis, Minn.
IV. P. J. Torvik, S. H. Chi, B. J. Lazan
V. Avail fr OTS
VI. In ASTIA collection